Biogeosciences Discuss., https://doi.org/10.5194/bg-2018-240
Manuscript under review for journal Biogeosciences
Discussion started: 27 June 2018


# Simulating the atmospheric $CO_2$ concentration across the heterogeneous landscape of Denmark using a coupled atmosphere-biosphere mesoscale model system

Anne Sofie Lansø[1,a], Thomas Luke Smallman[2,3], Jesper Heile Christensen[1,4], Mathew Williams[2,3], Kim Pilegaard[5], Lise-Lotte Sørensen[4], and Camilla Geels[1]

[1]Department of Environmental Science, Aarhus University, Frederiksborgvej 399, 4000 Roskilde, Denmark
[2]School of GeoSciences, University of Edinburgh, Edinburgh, EH9 3JN, UK
[3]National Centre for Earth Observation, University of Edinburgh, Edinburgh, EH9 3JN, UK
[4]Arctic Research Centre (ARC), Department of Bioscience, Aarhus University, Ny Munkegade 114, 8000 Aarhus, Denmark
[5]Department of Environmental Engineering, Technical University of Denmark (DTU), Bygningstorvet 115, 2800 Kgs. Lyngby, Denmark
[a]Now at: Laboratoire des Sciences du Climat et l'Environnement, LSCE/IPSL, CEA-CNRS-UVSQ, Université Paris-Saclay, 91191 Gif-sur-Yvette, France

*Correspondence to:* Anne Sofie Lansø (anne-sofie.lanso@lsce.ipsl.fr)

**Abstract.** Surface heterogeneity can be challenging to fully encompass by modelling studies of $CO_2$ surface exchanges, especially when it comes to land-sea boarders. The relative importance of the marine and the terrestrial surface fluxes on the atmospheric $CO_2$ concentration were examined by developing a mesoscale modelling framework capable of simulating surface exchanges at a high spatiotemporal resolution. This study exploits the complexity of the Danish landscape and the many land-sea boarders found along the nation's 7,300 km of coastline.

An atmospheric transport model, DEHM, with a horizontal spatial resolution of 5.6 km $\times$ 5.6 km constituted the basis of the modelling framework. A mechanistic biosphere model, SPA, was coupled to DEHM in order to simulate terrestrial surface exchanges applying a tiling approach with the seven most dominant land-use classes in Denmark to account for sub-grid heterogeneity. Detailed surface fields of $pCO_2$ were used to simulate the air-sea $CO_2$ exchange for the study region. Monthly mean diurnal cycles of surface water $pCO_2$ were imposed onto these, in order to include short-term variability in surface water $pCO_2$.

The Danish biospheric fluxes simulated by the SPA-DEHM model system experienced an east-west gradient corresponding to the distribution of the land-use classes and their biological activity. The relative importance of the seven land-use classes varied throughout the year according to their individual growth patterns. A major contribution to the monthly net ecosystem exchange (NEE) through all seasons came from grasslands, while the influence from croplands increased from March to July. Grasslands had, on an annual basis, the largest impact on the biospheric net uptake with -1,423 GgC $yr^{-1}$.

The total Danish biospheric uptake for 2011 was -6,302 GgC $yr^{-1}$. Relating the annual natural biospheric surface fluxes to the $CO_2$ emitted by fossil fuel combustions and industrial processes by Denmark, the Danish terrestrial uptake corresponded to 52 % of these, while the Danish annual marine uptake was negligible in comparison, although hiding larger seasonal variations.

Biogeosciences Discuss., https://doi.org/10.5194/bg-2018-240
Manuscript under review for journal Biogeosciences
Discussion started: 27 June 2018


During 2013-2014, the simulated atmospheric $CO_2$ concentrations compared well with measurements made at the Risø tall tower located on the shore of Roskilde Fjord ( R = 0.88 and RMSE = 4.87 ppm). The origin of the simulated $CO_2$ concentrations at Risø varied between seasons with biospheric fluxes and fossil fuel emissions having the largest impact on the variations. Impact from Roskilde fjord was difficult to detect in the simulated $CO_2$ concentrations. These difficulties in simulating the local impact from the Roskilde Fjord might arise from *(i)* the fjord not being adequately resolved in the constructed model system, *(ii)* the lack of a realistic representation of the surface water $pCO_2$ dynamics, or *(iii)* that the fjord is not in the simulated footprint and only had a modest impact on the simulated atmospheric $CO_2$ at the Risø tall tower.

## 1 Introduction

To have the best chance of accurately predicting the future evolution of the carbon cycle, and its implications for our climate, it is important to eliminate, or at least minimise, the uncertainty that exists in the present estimates. Enhanced knowledge, improved temporal resolution of surface exchange processes and improvements in the spatial surface representation are factors that could minimise these uncertainties.

On an annual basis the biosphere is estimated to absorb $3.0 \pm 0.8$ PgC yr$^{-1}$ of the $9.4 \pm 0.5$ PgC yr$^{-1}$ anthropogenic carbon emitted to the atmosphere (Le Quéré et al., 2018). The heterogeneity and the dynamics of the land surface complicates such estimates. Biosphere models of various complexity have been developed to spatially simulate surface fluxes of $CO_2$, but global bottom-up estimates are poorly constrained by surface observation. Although a huge observational effort has been and is still being put into observing surface exchanges, the observations are far from a global surface representation (Ciais et al., 2014; Zscheischler et al., 2017).

In order to omit the lack of surface observation, atmospheric models have been used to construct inverse modelling systems, where atmospheric $CO_2$ measurements have been used to constrain surface fluxes (e.g. Baker et al. (2006); Gurney et al. (2002, 2004); Peylin et al. (2013)). These atmospheric inversions are capable of capturing the year to year changes in natural surface fluxes, the magnitude and distribution of regional fluxes, and distinguish between land and ocean fluxes (Le Quéré et al., 2015). However, atmospheric inversions are limited by the availability of atmospheric measurements, and therefore, only regional inversions have been conducted in areas with very dense data network, e.g, Europe (Broquet et al., 2011; Rödenbeck et al., 2009), the corn belt of the United States (Lauvaux et al., 2012), and national scale inversions for the Netherlands (Meesters et al., 2012; Tolk et al., 2011).

Studying surface exchanges of $CO_2$ on regional to local scale can be accomplished with mesoscale atmospheric transport models. Their resolution is in the range from 2 km to 20 km and their advantage is their capability to get a better processes understanding of both atmospheric and surface exchange mechanisms in order to improve the link between observations and models at all scales, i.e. for both mesoscale, regional and global models (Ahmadov et al., 2007). The higher spatial resolution of mesoscale models allows for a better representation of atmospheric flows and for a more detailed surface description, which in particular for heterogeneous areas is advantageous. In previous mesoscale model studies, biosphere models have been coupled to the mesoscale atmospheric models ranging in their complexity from simple diagnostic (Sarrat et al., 2007b; Ahmadov et al., 2007, 2009) to mechanistic process based biosphere models (Tolk et al., 2009; Ter Maat et al., 2010; Smallman et al., 2014; Uebel et al., 2017). The modelled $CO_2$ concentrations and surface fluxes from mesoscale model systems compare better with observations than global model systems (Ahmadov et al., 2009). The atmospheric impact on surface processes related to the ecosystem's sensitivity and $CO_2$ exchange can be examined in greater details (Tolk et al., 2009) and tall towers footprints can be studied more concisely (Smallman et al., 2014).

The heterogeneity of coastal ocean contributes with a large uncertainty to assessment of the air-sea $CO_2$ exchange (Regnier et al., 2013). Coastal seas, rich in nutrient and organic material, might contribute with an in-proportional amount to the global air-sea $CO_2$ flux, with regards to its limited spatial area when compared to the open oceans (Gattuso et al., 1998). The observed high spatial and temporal variability (Kuss et al., 2006; Leinweber et al., 2009; Vandemark et al., 2011; Norman et al., 2013; Mørk et al., 2016) are not always included in marine models (Omstedt et al., 2009; Gypens et al., 2011; Kuznetsov and Neumann, 2013; Gustafsson et al., 2015; Valsala and Murtugudde, 2015), let alone taken into account in atmospheric mesoscale systems simulating $CO_2$ (Sarrat et al., 2007a; Geels et al., 2007; Law et al., 2008; Tolk et al., 2009; Broquet et al., 2011; Kretschmer et al., 2014). Moreover, a recent study has found that short-term variability in the partial pressure of surface water $CO_2$ ($pCO_2$) can be very influential of the annual flux for some coastal areas (Lansø et al., 2017).

In this study we aim to simulate surface exchanges of $CO_2$ at a high spatial-temporal resolution together with mesoscale atmospheric transport. Interactions between the atmosphere - ocean, and atmosphere - biosphere are contained in a mesoscale modelling framework together with high resolution anthropogenic emissions of $CO_2$. The study area comprises of Denmark, a country that is characterised by a varied land mosaic containing urban, forest and agricultural areas. With more than 7,300 km of coastline encircling approximately 43,000 km$^2$ of land, many land-sea borders are found throughout the country adding to the complexity. The developed mesoscale modelling system is used to assess and understand the dynamics and relative importance of the marine and terrestrial $CO_2$ fluxes across this particular region with a special focus on the impact from the Roskilde Fjord system. The Danish Eulerian Hemispheric Model, DEHM, forms the basis of the framework, while the mechanistic biospheric Soil-Plant-Atmosphere model, SPA, is dynamically coupled to the atmospheric model. The air-sea $CO_2$ exchange is simulated at a high temporal resolution with the best applicable surface fields of $pCO_2$ for the Danish marine areas. Tall tower observations are used to evaluate the simulated atmospheric concentrations of $CO_2$.

## 2 Model setup

The model framework used in the present study consists of two models; DEHM and SPA. A coupling between the two was made for the inner most nest of DEHM in order to simulate the exchange of $CO_2$ between the atmosphere and terrestrial biosphere at a high temporal (1 hour) and spatial resolution (5.6 km × 5.6 km) for the area of Denmark.

### 2.1 DEHM

DEHM is an atmospheric chemical transport model covering the Northern Hemisphere with a polar stereographic projection true at 60°N. Originally, developed to study sulphur and sulphate (Christensen, 1997), the DEHM model now contains 58 chemical species and nine groups of particular matter (Brandt et al., 2012). This adaptable model has been used to study such different things as atmospheric mercury (Christensen et al., 2004), persistent organic pollutants (Hansen et al., 2004), biogenic volatile organic compounds influence on air quality (Zare et al., 2014), emission and transport of pollen (Skjøth et al., 2007), ammonia and nitrogen deposition (Geels et al., 2012a, b) and atmospheric $CO_2$ (Geels et al., 2002, 2004, 2007; Lansø et al., 2015). The $CO_2$ version of DEHM was used in the present study. DEHM has 29 vertical levels distributed from the surface to the 100 hPa surface, and horizontally 96 × 96 grid points, which through it's nesting capabilities increases in resolution from 150 km × 150 km in the main domain to 50 km × 50 km, 16.7 km × 16.7 km and 5.6 km × 5.6 km in the three nests.

### 2.1.1 Inputs to DEHM

Anthropogenic emissions of $CO_2$, wild fire emissions and optimized biospheric fluxes from NOAAs ESRL Carbon Tracker system (Peters et al., 2007) version CT2015 were used as inputs to DEHM. Their resolution is $1° \times 1°$ with updated values every third hour. Similarly, CT2015 three-hourly molefractions of $CO_2$ were used as boundaries conditions towards the Southern Hemisphere.

Hourly anthropogenic emissions on a 10 km × 10 km grid from the Institute of Energy Economics and the rational Use of Energy (IER, Pregger et al. (2007)) were applied for Europe instead of emissions from CT2015. Furthermore, these are for the area of Denmark substituted by hourly anthropogenic emissions with an even higher spatial resolution of 1 km × 1 km (Plejdrup and Gyldenkærne, 2011). As the European and Danish emission inventories were from 2005 and 2011, respectively, the emissions were scaled to annual national total $CO_2$ emission of fossil fuel and cement production conducted by EDGAR (Olivier et al., 2014), in order to include the yearly variability in national anthropogenic $CO_2$ emissions.

The necessary meteorological parameters for DEHM were simulated by the Weather Research and Forecast Model (WRF) (Skamarock et al., 2008), nudged by six hourly ERA-Interim meteorology, which was also used as initial and boundary conditions (Dee et al., 2011).

### 2.1.2 Air-sea $CO_2$

The exchange of $CO_2$ between the atmosphere and the ocean, $F_{CO_2}$, was calculated by $F_{CO_2} = K k_{660} \Delta pCO_2$, where $K$ is solubility of $CO_2$ calculated as in Weiss (1974), $k_{660}$ is the transfer velocity of $CO_2$ normalised to a Schmidt number of 660 at 20°C, and $\Delta pCO_2$ is the difference in partial pressure of $CO_2$ between the surface water and the overlying atmosphere. The transfer velocity parameterisation $k = 0.266 u_{10}^2$, where $u_{10}^2$ is the wind speed at 10 m, determined by Ho et al. (2006) has been found to match Danish fjord systems (Mørk et al., 2016), and was applied in the current study. Surface values of marine $pCO_2$ were described by a combination of the open ocean surface water climatology of $pCO_2$ by Takahashi et al. (2014), and the climatology developed by Lansø et al. (2015, 2017) for the Baltic Sea and Danish waters. Furthermore, short-term temporal variability was accounted for in the surface water $pCO_2$ by imposing monthly mean diurnal cycles onto the monthly climatologies following the method described in Lansø et al. (2017).

Biogeosciences Discuss., https://doi.org/10.5194/bg-2018-240
Manuscript under review for journal Biogeosciences
Discussion started: 27 June 2018


### 2.2 SPA

The SPA model is a mechanistic terrestrial biosphere model (Williams et al., 1996, 2001). SPA has a high vertical resolution with up to 10 canopy layers (Williams et al., 1996) allowing for variation in the vertical profile of photosynthetic parameters and multi-layer turbulence (Smallman et al., 2013). Within the soil up to 20 soil layers can be included (Williams et al., 2001). The radiative transfer scheme estimates the distribution of direct and diffuse radiation, and sunlit and shaded areas (Williams et al., 1998). SPA uses the mechanistic Farquhar model (Farquhar and von Caemmerer, 1982) of leaf level photosynthesis, and the Penman-Monteith model to represent leaf level transpiration (Jones, 1992). Photosynthesis and transpiration are coupled via a mechanistic model of stomatal conductance, where stomatal opening is adjusted to maximise carbon uptake per unit nitrogen within hydraulic limitations, determined by a minimum leaf water potential tolerance, to prevent cavitation.

Ecosystem carbon cycling and phenology is determined by a simple carbon cycle model (DALEC, Williams et al. (2005), which is directly coupled into SPA. DALEC simulates carbon stocks in foliage, fine roots, wood (branches, stem and coarse roots), litter (foliage and fine root) and soil organic matter (including coarse woody debris). Photosynthate is allocated to autotrophic respiration and living biomass via fixed fractions, while turnover of carbon pools is governed by first order kinetics. In addition, when simulating crops, a storage organ (i.e. the crop yield) and dead, but still standing, foliage pools are added (Sus et al., 2010).

SPA has been extensively validated against site observations from temperate forests (Williams et al., 1996, 2001), temperate arable agriculture (Sus et al., 2010) and Arctic tundra (Williams et al., 2000). SPA has more recently been coupled into the Weather Research and Forecasting (WRF) model (Skamarock et al., 2008), the resulting WRF-SPA model was used in multi-annual simulations over the United Kingdom and assessed against surface fluxes of $CO_2$, $H_2O$ and heat, and atmospheric observations of $CO_2$ from aircraft and a tall tower (Smallman et al., 2013, 2014).

SPA needs vegetation and soil input parameters. Initial soil carbon stock estimates were obtained from the Regridded Harmonized World Soil Database (Wieder, 2014). The vegetation inputs and plant traits for SPA were partly taken from previous parameter sets used in SPA, but also from the Plant Trait Database (TRY, Kattge et al. (2011)), and from literature (Penning de Vries et al., 1989; Wullschleger, 1993). As these parameters and plant traits were determined at various sites that not necessarily corresponds to Danish conditions, a calibration of the vegetation inputs to SPA was conducted for Danish Eddy Covariance (EC) flux sites (Table 1). Only data from five sites were available and these were divided in two sets – one for calibration (all available observations before 2013), the other validation (all available observations from 2013 and 2014).

#### 2.2.1 SPA calibration

The calibration was conducted by selecting a set of inputs parameters (plant traits, carbon stocks etc.) and for each parameter five values within a realistic range were chosen. Next, 200 SPA simulations with randomly chosen parameter values were conducted. These results were statistically evaluated against observations of net ecosystem exchange (NEE) from the different flux sites, and the simulations with the lowest root mean square error (RMSE) in combination with highest correlation were selected. Based on this random parameter testing, it was possible to choose the best set of realistic vegetation input parameters that could improve the model performance at the Danish sites. The best found vegetation parameters values corresponded in some cases to the values already applied in SPA for the given land cover.

#### 2.2.2 Validation

Comparing to observations of NEE, SPA was, in general, able to capture the phenology and seasonal cycle throughout the entire simulation period (Fig. 1). Correlations and RMSEs between the model and the independent data from the validation period (Fig. 1) likewise indicate a good model performance. At Sorø both variability, as inferred from the standard deviations, the amplitude and the onset of the growing season were well reproduced by the SPA model. However, difficulties with simulating the evergreen forest at Gludsted is evident with more variation modelled than given by the observations, and a lag of the start of the growing season when compared to the observations. The evergreen plant functional type in SPA experiences phenological problems with rapid leaf growth in response to environmental drivers, which causes a delay in spring photosynthesis. Voulund alternates between winter and spring barley for the calibration period starting with winter barley in 2009. Note that the whole observed time series of NEE at Voulund is shown together with model NEE of both winter and spring barley (Fig. 1c and d). While the phenology and amplitude are well captured by spring barley at Voulund, SPA is not able to capture the seasonal amplitude of the winter barley that seems to be more sensitive to the meteorological drives, and seasons with harder winters had lower NEE peaks in summer. At the grassland site Skjern Enge, NEE is for winter, spring, and the first part of the summer reasonably modelled. The difficulties for late summer and autumn arise from the management practises at the site, where both grazing and grass cutting are conducted, limiting NEE (Herbst et al., 2013). Although grazing is included in the SPA model, it does not simulate the same reduction in NEE.

In the inner most nest of DEHM for the area of Denmark, a coupling was made between DEHM and SPA. Thus, the coarser optimized biospheric fluxes from CT2015 were for Denmark replaced by hourly SPA simulated $CO_2$ fluxes. With this change, the spatial resolution for the biosphere fluxes was increased from $1° \times 1°$ to 5.6 km $\times$ 5.6 km allowing for a better representation of the Danish surface, and hence also the biospheric fluxes.

A tiling approach with seven most common biospheric land-use classification were selected for this study including deciduous forest, evergreen forest, winter wheat and other winter crops, winter barley, spring barley and other spring crops, grassland and agricultural other, but excluding urbanised areas. This classification corresponds to the actual crop distribution of 2011 (Jepsen and Levin, 2013). Denmark is dominated by agriculture, and more than 60 % of the used classification is agricultural land. DEHM provides on an hourly basis meteorological drivers and atmospheric $CO_2$ concentrations to SPA, while SPA each hour returns NEE to DEHM.

### 2.3 Observations of atmospheric $CO_2$

Tall tower continuous measurements of atmospheric $CO_2$ concentrations made by a Picarro 118 m above the surface have been conducted at the Risø site since the middle of 2013. The Risø site is located on the eastern inner shore of Roskilde Fjord (55°41′N, 12°05′E), Zealand, which is a narrow microtidal estuary 40 km long with a surface area of 123 km$^2$ and a mean depth of 3 m (Mørk et al., 2016).

Biogeosciences Discuss., https://doi.org/10.5194/bg-2018-240
Manuscript under review for journal Biogeosciences
Discussion started: 27 June 2018


## 3 Results

The model system was run from 2008 to 2014, however, the first three years were regarded as a spin-up period. Given that the land-use classification corresponds to the actual distribution of 2011 an emphasis will be put on the terrestrial fluxes for this particular year during the analysis together with an estimation of the annual Danish carbon budget. Measurements of atmospheric $CO_2$ will be used to assess the performance of the DEHM-SPA model system, and evaluate local impacts from fjord systems on atmospheric $CO_2$ concentrations.

### 3.1 Surface fluxes

#### 3.1.1 Biospheric fluxes

Across Denmark, there is an east-west gradient in the simulated biospheric fluxes of carbon for both January and July in 2011. Larger fluxes of gross primary productivity (GPP), ecosystem respiration and NEE are evident in the western part of Denmark, while the islands and Eastern Jutland have lower biosphere fluxes (Fig. 2). This gradient follows the distribution of the individual land-use classifications (Appendix A Fig. A1) and their grow patterns, but also reflects the population density which is highest in the eastern part of the country.

Table 2 and Table 3 show the contribution of each individual land-use class to the total GPP and respiration on a national scale (see Appendix B Table B1 - B3 for monthly GPP, respiration and NEE per land-use class). The monthly contributions to the country-wide total inherently reflect the total area for each land-use class. In winter, GPP is highest for evergreen, grassland and agricultural other. These land-use classes are well represented in Western Jutland explaining why the largest biological production is found here during January (Fig. 2a). As the crops develop, their contribution to the total monthly GPP increases, and in July winter crops are together with grasslands the most productive land-use classes. Also, deciduous forest increases its share of GPP from the onset of the growing season, but as its spatial extent only amount to 10 %, its monthly contribution is never dominant. Respiration is less concentrated for individual land-use classes and the individual monthly contributions vary much less for respiration than GPP throughout the year, though with a notable increase in contribution from both winter and spring crop through spring and summer until harvest (Table 3). The highest contributions of respiration are throughout the year found for grassland and agriculture other.

Integrating over all land-use classes for 2011, the Danish terrestrial land surfaces is net source of $CO_2$ to the atmosphere in the months from January to April, and October to December, with the highest monthly release of 1,129 GgC month $yr^{-1}$ in December. From May to September, the biosphere is a net sink with a maximum uptake in June of -4,687 GgC month $yr^{-1}$. The total annual surface exchange of $CO_2$ between the atmosphere and Danish biosphere is -6,302 GgC $yr^{-1}$ for 2011, where grassland has the largest contribution with -1,423 GgC $yr^{-1}$.

#### 3.1.2 Marine fluxes

The air-sea $CO_2$ exchange in the Danish inner waters experiences large seasonal variations, while the variations in the North Sea are less pronounces as illustrated by Fig. 3. Bordering the Baltic Sea, the Danish inner waters are rich on nutrients and organic material (Kuliński and Pempkowiak, 2011). This fosters high biological activity in spring and summer lowering surface water $pCO_2$ allowing for uptake of atmospheric $CO_2$. In winter, mineralisation increases $pCO_2$ (Wesslander et al., 2010), and outgassing of $CO_2$ to the atmosphere takes place. The North Sea is a continuously sink of atmospheric $CO_2$, where a continental shelf-sea pump removes $pCO_2$ from the surface water and transport it to the North Atlantic Ocean (Thomas et al., 2004).

To estimate the annual exchange of $CO_2$ between the atmosphere and the ocean for the Danish marine areas, the exclusive economic zone (EEZ) is used. In the EEZ the coastal state (in this case Denmark) has the right to explore, exploit and manage all resources found within it (United Nations Chapter XXI: Law of the Sea, 1984). Thus, assuming the air-sea $CO_2$ exchange counts as a natural resource for Denmark, the air-sea flux from EEZ was used for the annual budget estimation of $CO_2$. The 2011 simulated annual air-sea $CO_2$ exchange in the 105,000 km$^2$ covered by the Danish EEZ amounts to -422 GgC yr$^{-1}$. However, this number hides large spatial differences and monthly numerical larger fluxes. While the North Sea area contained within the EEZ continuously had monthly uptakes in the range -73 GgC mon$^{-1}$ to -191 GgC mon$^{-1}$, the monthly fluxes from the near coastal (marine areas extending up to 10 km of shore) Danish inner waters varied in the range -46 GgC mon$^{-1}$ to 540 GgC mon$^{-1}$.

#### 3.1.3 Danish $CO_2$ budget

The annual $CO_2$ budget for year 2011 is assessed, because the crop distribution used for the land-use classification was based on data from this specific year as was the spatial distribution of the Danish fossil fuel emissions. In 2011, Denmark emitted 12,205 GgC yr$^{-1}$ of $CO_2$ to the atmosphere due to fossil fuel combustion and industrial processes (Nielsen et al., 2015). The Danish terrestrial biosphere took up -6,302 GgC yr$^{-1}$ of $CO_2$ during 2011, which equals 52 % of the $CO_2$ emitted by anthropogenic activity in Denmark. The marine uptake of -422 GgC yr$^{-1}$ is annually less influential and corresponds to only 3.5 % of the anthropogenic emitted $CO_2$.

### 3.2 Atmospheric $CO_2$ concentrations

The time series of measured and simulated $CO_2$ show good agreements (Fig. 4) with R = 0.88 and RMSE = 4.87 ppm for daily averaged time series demonstrating that the model is capable of capturing the synoptic scale variability. Also, good statistical measures are obtained for the hourly time series with R = 0.84 and RMSE = 5.95 ppm, but the short-term variability is not always fully captured by the model. Overall the model simulates the atmospheric $CO_2$ quite well, indicating that the simulated surface exchange of $CO_2$ is acceptable.

To investigate the origin of the $CO_2$ simulated at the Risø site, concentration rose plots of simulated atmospheric $CO_2$ have been made (Fig. 5). The concentration rose shows the wind direction and associated $CO_2$ concentrations. Roskilde Fjord lies

Biogeosciences Discuss., https://doi.org/10.5194/bg-2018-240
Manuscript under review for journal Biogeosciences
Discussion started: 27 June 2018


in the approximate sector of 200°- 360°relative to the Risø tower, the city of Roskilde (with 50,000 inhabitants) is positioned approximately 5 km south to south-west of the tower, while Copenhagen lies 20 km east. Division has been made between seasons, and day and night time values both showing distinct seasonal and diurnal patterns. The highest values of $CO_2$ are obtained during winter, where very little diurnal variation is seen. During summer the lowest values are obtained in particular during daylight, when photosynthesis occurs.

The individual contribution from fossil fuel emissions, marine and biospheric exchanges to the atmospheric $CO_2$ (see Appendix C Fig. C1 - C3) indicate that the biosphere contributes most to the variations simulated at Risø (Fig. C2) – both seasonally and daily. Emissions of fossil fuel experience little diurnal variability, but seasonally with the greatest contribution during autumn and winter (Fig. C1). Highest values are seen originating from the sectors encapsulating the city of Roskilde and the capital region. In all seasons, the simulated oceanic contribution is negative, i.e. indicating uptake of atmospheric $CO_2$, but the marine contribution is small with little variation (Fig. C3). The less negative values in autumn and winter may be a result of the simulated outgassing of $CO_2$ from the Baltic Sea and Danish inner waters during the winter season (Lansø et al., 2015), which however is still dominated by the uptake by global open oceans.

The local impact from Roskilde Fjord is difficult to detect in the marine concentration plots. Flux measurements at Roskilde Fjord have shown uptake of $CO_2$ during spring, while release in the remaining seasons (Mørk et al., 2016), which is accurately captured by the modelling system (Lansø et al., 2017). A footprint analysis of the Risø tower has shown that the fluxes from Roskilde Fjord has a contribution to the total $CO_2$ flux measured at the top of the 118 m high tower, but only minor, since fluxes over water typically is an order of magnitude smaller than fluxes over land (Sogachev and Dellwik, 2017). Therefore, we investigated a period with observed large outgassing from Roskilde Fjord - a storm event in October 2013 that was observed to increase the monthly release of $CO_2$ in the fjord by 66 % (Mørk et al., 2016). The storm event passed Denmark on 28 October 2013, and at 06 UTC southerly winds transport air masses with higher $CO_2$ towards the Risø site (Fig. 6a), while at the same time a detectable increase in the oceanic contribution to the $CO_2$ concentration at the Roskilde Fjord system is seen (Fig. 6b). The model system simulates the small peak in the observed atmospheric $CO_2$ concentrations for 28 October (Fig. 7a) at the Risø site, but distinguishing between contributions from fossil fuel emissions, the biosphere and the ocean to the atmospheric $CO_2$ concentration at Risø (Fig. 7b) reveals no oceanic impact, and hence no apparent influence from Roskilde Fjord during the storm event.

## 4 Discussion

### 4.1 Biospheric fluxes

Spatially, the Danish biospheric fluxes of $CO_2$ follows the land-use classification that mirrors the population density being highest in eastern and lowest in western Denmark. While GPP follows phenology and productivity resulting in changing percentage contribution from the land-use classes to the monthly total GPP, the mutual proportions of respirations are much less varied. Autotropic respiration depends on plant productivity, but the heterotropic respiration is temperature dependent and will change proportionally for each land-use class maintaining a more constant percentage-wise distribution.

Biogeosciences Discuss., https://doi.org/10.5194/bg-2018-240
Manuscript under review for journal Biogeosciences
Discussion started: 27 June 2018


The simulated annual uptake by deciduous forest of -300 gC $m^{-2}$ $yr^{-1}$ for 2011, fits the observed range of annual estimated NEE at Sorø from 1996 to 2009 spanning 32 gC $m^{-2}$ $yr^{-1}$ to -331 gC $m^{-2}$ $yr^{-1}$ (Pilegaard et al., 2011). Even though SPA experiences a lag in the seasonal onset for the evergreen forest, the annual estimated uptake of -386 gC $m^{-2}$ $yr^{-1}$ compares well with previous estimates of temperate evergreen forests with -402 gC $m^{-2}$ $yr^{-1}$ (Luyssaert et al., 2007) and Danish evergreen plantations of -503 gC $m^{-2}$ $yr^{-1}$ (Herbst et al., 2011). However, improvements to the evergreen plant functional type in SPA are needed, and an addition of a labile pool to the evergreen carbon assimilation would omit the seasonal lag (Williams et al., 2005). Such adjustments have already been made to the DALEC carbon assimilation system utilised by SPA (Smallman et al., 2017), but not yet incorporated into SPA.

Previous annual estimates at Danish agricultural field sites found carbon uptake with -31 gC $m^{-2}$ $yr^{-1}$ estimated from a mixed agricultural landscape (Soegaard et al., 2003) and -245 gC $m^{-2}$ $yr^{-1}$ from winter barley (Herbst et al., 2011). The SPA-DEHM model system simulated annual uptakes for winter wheat and spring crops of -137 gC $m^{-2}$ $yr^{-1}$ and -207 gC $m^{-2}$ $yr^{-1}$, respectively, and thus fits the previous estimates well, while winter barley had a small release of 32 gC $m^{-2}$ $yr^{-1}$. The calibration and validation (1c) shows difficulties in simulating the observed NEE during growing seasons for winter barley particularly after cold and snow covered winters (winter 2010-11, 2012-13). For 2011 winter barley had the smallest total area of the agricultural land-use classifications, and was dominated by the respiration. As pointed out in previous studies, the crop modelling component in SPA could likewise be improved e.g. inclusion of intra-seasonal crops (Smallman et al., 2014).

The current study annually estimated the Danish grasslands to be a sink of $CO_2$ with -205 gC $m^{-2}$ $yr^{-1}$, which are similar to the -267 gC $m^{-2}$ $yr^{-1}$ observed at the Skjern Enge grassland site(Herbst et al., 2011) and the -312 gC $m^{-2}$ $yr^{-1}$ observed at the Lille Valby grassland site, Denmark (Gilmanov et al., 2007). The European grassland study by Gilmanov et al. (2007) found large variation in annual fluxes from grassland driven by environmental conditions and management practises at the sites varying from 171 gC $m^{-2}$ $yr^{-1}$ to -707 gC $m^{-2}$ $yr^{-1}$, but with most site having an annual uptake of carbon. As seen in Fig. 1e more work on grassland calibration could have been done, but the conditions and management regimes at Skjern Enge does not necessarily fit the rest of the Danish grassland. With the chosen parameters, very comparable results were obtained indicating that such an additional calibration might not be advantageous.

A tilling approach has been used for the land-use classification in the SPA-DEHM modelling framework, including sub-grid heterogeneity in the model system. However, the seven land-use classes do not fully encompass the ecosystem variability in Denmark. Both grassland and agricultural other cover a broad range of sub-categories with both heather and meadow included in the grassland class, while agricultural other among other things contains vegetables fields, hedgerows, woodland patches and uncultivated land. Moreover, large urbanised areas are not accounted for in the current classes either. Adding more land-use classifications could give a better and more realistic surface description, if data for both calibration of validation for the lacking land-use classes, preferably from similar climatic region as Denmark, were available.

### 4.2 National $CO_2$ budget

The current estimate of the global carbon budget appraises the global biosphere to take up 32 % of the $CO_2$ emitted by fossil fuel and industry, while the global oceans are estimated to take up 26 % (Le Quéré et al., 2018). National scale biospheric uptakes can vary greatly between countries depending on land coverage, land-use and management practices (Janssens et al., 2005). Meesters et al. (2012) estimated an annual biospheric uptake for the Netherlands of -17,400 GgC $yr^{-1}$ (approximately -497 gC $m^{-2}$ $yr^{-1}$), which corresponded to 33 % of the annual fossil fuel emitted by the country. An annual uptake of -99 gC $m^{-2}$ $yr^{-1}$ has been estimated for Scotland by Smallman et al. (2014). The current study estimates a total annual biospheric uptake of -6,302 Gg C $yr^{-1}$, which equals 52 % of the $CO_2$ emitted by anthropogenic activities in Denmark. Integrating over all land-use classes the uptake per area is -195 gC $m^{-2}$ $yr^{-1}$, which places this Danish estimate within the bounds of the previous national estimates at similar latitudes. Caution should be taken when assessing the Danish $CO_2$ budget. We present a one year snap-short of the state of the Danish surface exchanges of $CO_2$, but important processes such as product use, biomass burning and river runoff linking land and ocean are lacking in our estimate in order to fully close the budget.

### 4.3 Atmospheric $CO_2$ and land-sea signals

The SPA-DEHM modelling system resembles the synoptic and diurnal variability in the atmospheric $CO_2$ concentrations measured at Risø site. The variability at the Risø site is dominated by the biospheric impact and fossil fuel emissions of $CO_2$. The signal from Roskilde Fjord is difficult to detect in the simulated $CO_2$ concentrations. Even when the marine contribution to the atmospheric concentration alone is examined, the Roskilde Fjord signal is hard to distinguish at the Risø tower. Rather the global and regional signals are obtained, e.g. the winter release of $CO_2$ from the Baltic Sea resulting in less negative values for the concentration rose plot. Even though the oceanic contribution to the atmospheric short-term variability is low, oceanic impact is still important on monthly and annual scale time scales. As the Roskilde Fjord by a footprint analysis previously was found to have an impact on the atmospheric $CO_2$ concentration at the top of the tower (Sogachev and Dellwik, 2017), a period with observations of large outgassing from Roskilde Fjord was examined to more clearly envisions its impact in the constructed modelling system. Both the simulated and observed atmospheric $CO_2$ increased during the storm event on October 28 (Fig. 6a), but no concurrent increase was seen for the oceanic contribution to atmospheric $CO_2$ at the Risø site (Fig. 6b). This might be explained by the southerly winds that transports the $CO_2$ released from the fjord northward and away from the Risø Tower, which is positioned in the southern part of the fjord. Moreover, in this study the increased flux from Roskilde Fjord was only caused by increased wind speed together with the impose diurnal cycle of marine $pCO_2$ (the diurnal amplitude for October was approximately 10 $\mu$atm), while measurements suggested that also an increase in surface water $pCO_2$ of approximately 300 $\mu$atm sustained the observed $CO_2$ flux (Mørk et al., 2016). The lack of such increase in surface water $pCO_2$ in the current modelling study, could explain why no impact on the simulated atmospheric $CO_2$ is seen from the marine component during the storm event.

Thus the results could indicate that *(i)* the narrow Roskilde Fjord was not sufficiently resolved in the current model framework, where the horizontal grid resolution is 5.6 km $\times$ 5.6 km, *(ii)* the surface water $pCO_2$ was not described in enough details in the model system, or *(iii)* Roskilde fjord is not in the footprint of the tower and thus only has a minor impact on the atmospheric $CO_2$ concentrations at Risø.

### 4.4 Uncertainties in relation to surface exchanges of $CO_2$

Some of the largest uncertainties lie in the parameters underlying the terrestrial carbon cycle, in particular those governing allocation to plant tissues and their subsequent turnover. Most often these are based on maps of land cover or plant functional type, but parameter estimation via data assimilation analysis has shown substantial spatial variation of terrestrial ecosystem parameters within plant functional type groupings with consequences for carbon cycling predictions (Bloom et al., 2016). Increasing the amount of observational data used in data assimilation system have been found to reduce uncertainty in retrieved parameters and thus simulated carbon stocks and fluxes of $CO_2$ (Smallman et al., 2017); including all observations counting both in situ and satellite, Smallman et al. (2017) halved the uncertainty of the net biome productivity. While SPA also uses DALEC to simulate carbon allocation and turnover, it is currently impractical to conduct a similar data assimilation analysis or to repeatedly simulate atmospheric transport to robustly quantify the impact of flux uncertainties on atmospheric $CO_2$ concentrations due to their computational requirements. While conducting such an analysis remains a future ambition we consider it to be out of scope for the current study, since the terrestrial surface fluxes in this study is constrained by one data stream consisting of EC measurements. This study has focused on surface fluxes over a relative short time period, and the model framework was capable of producing such fluxes a satisfactorily level, including their aggregated impact on atmospheric $CO_2$ concentrations (Fig. 4) with R = 0.88 and RMSE = 4.87 ppm for daily values. The usage of satellite retrievals by data assimilations systems and their accompanying improvements moreover highlights the future enhancement to the current modelling framework, where satellite products could be utilized for upscaling reducing the related error.

Uncertainties of the marine fluxes can be associated with both the choice of transfer velocity parameterisation, choice of wind speed product and the used surface water $pCO_2$ maps. Sensitivity analysis of global transfer velocity parameterisation based on $^{14}C$ bomb inventories shows uncertainties of 20 %, while varying the applied wind speed products for these formulation increase the difference in the global annual flux by 40 % (Roobaert et al., 2018). Including empirical formulations of transfer velocity parameterisation in the analysis increase the sensitivity to wind speed product to nearly 70 %, while the uncertainty to the parameterisation itself is more the 200 %. More than a doubling of the annual uptake by the usage of different transfer velocity formulations has likewise been shown for the study region (Lansø et al., 2015), while the choice of surface map could change the study region from an annual sink to source of atmospheric $CO_2$ (Lansø et al., 2017) As shown by Roobaert et al. (2018) the ERA-Interim and the transfer velocity formulation by Ho et al. (2006) used in the present study have a combined uncertainty estimate around 20 %. The improved data-driven near coastal Danish $pCO_2$ climatology better reflects the observed spatial dynamics and seasonality in the Danish inner waters (Mørk, 2015), albeit not diminishing the uncertainty related to surface maps of $pCO_2$ but reducing it.

## 5 Conclusions

By usage of the designed mesoscale modelling framework, it was possible to get a detailed insight into the spatio-temporal variability of the Danish surface exchanges of $CO_2$. The simulated biospheric fluxes experienced an east-west gradient corresponding to the distribution of the land-use classes and their biological activity. The relative importance of the seven land-use classes varied throughout the course of the year. In general, grasslands had a high contribution to the monthly NEE through all seasons, while crop-lands influence grew from March to July. On an annual basis, grasslands had the largest impact on the biospheric uptake with -1,423 GgC $yr^{-1}$.

The 12,205 GgC $yr^{-1}$ of $CO_2$ emitted by Danish fossil fuel during 2011 is comparable to almost double the uptake by the Danish land and marine areas with a biospheric uptake of 52 % and marine uptake corresponding to a few percent. The Danish total annual biospheric uptake was not unreasonable, when compared to other national scale annual estimates. However, the biospheric uptake could benefit both from model improvement and divisions into more land-use classes.

Good accordance between simulated and observed concentrations was found between modelled and observed atmospheric $CO_2$ concentrations for 2013 and 2014 at the Risø site. The origin of the modelled $CO_2$ concentrations at Risø varied with biospheric fluxes having the largest impact on diurnal variability, while on a seasonal scale fossil fuel emissions also had a dominant role. The local impact from Roskilde Fjord was difficult to detect, while regional impact from the Baltic Sea and Danish inner Straits are apparent in winter. The results may indicate that Roskilde Fjord and its localised impact (i.e. at the Risø site) on atmospheric $CO_2$ is not adequately resolved in the current model set-up or only have modest effect.

In order to further examine the air-sea signal at the complex Risø site surrounded by a mosaic of fjord systems, land masses and the Danish inner water, more model experiments could be made, where a bigger focus was put on other marine areas than Roskilde Fjord as e.g. the Danish Inner Straits, Kattegat and the Baltic Sea. Although the total annual marine flux was small, it disguises large monthly variations, and further investigations could help to understand the carbon dynamics in coastal regions. A runoff component in the modelling system would moreover be beneficial for such studies.

*Code availability.* Scientist with an interset in the atmospheric chemical transport model, DEHM, can contact Jesper H. Christensen (jc@envs.au.dk) with enquiries. Scientist with an interest in the Soil-Plant-Atmosphere model, SPA, can visit its webpage (https://www.geos.ed.ac.uk/homes/mwilliam /spa.html) or contact Mathew Williams (mat.williams@ed.ac.uk).

**Appendix A: Land-use classification**

**Appendix B: Biospheric fluxes**

**Appendix C: Concentration Roses**

*Competing interests.* The authors declare that there is no competing interests.

*Acknowledgements.* This study was carried out as part of a PhD study within the Danish ECOCLIM project funded by the Danish Strategic Research Council (Grant no. 10-093901). CarbonTracker CT2015 results provided by NOAA ESRL, Boulder, Colorado, USA from the website at http://carbontracker.noaa.gov have contributed to this work. Emissions inventories form IER, EDGAR and Aarhus University have likewise had an important contribution. This study has been supported by the TRY initiative on plant traits (http://www.try-db.org). The TRY initiative and database is hosted, developed and maintained by J. Kattge and G. Bönisch (Max Planck Institute for Biogeochemistry, Jena, Germany). TRY is currently support by DIVERSITAS/Future Earth and the German Centre for Integrative Biodiversity Research (iDiv) Halle-Jena-Leipzig. Moreover, this work used eddy covariance data acquired and shared by the Danish HOBE Center for Hydrology - Hydrological Observatory fonded by the Villum Foundation and by the FLUXNET community. The FLUXNET eddy covariance data processing and harmonization was carried out by the European Fluxes Database Cluster, AmeriFlux Management Project, and Fluxdata project of FLUXNET, with the support of CDIAC and ICOS Ecosystem Thematic Center, and the OzFlux, ChinaFlux and AsiaFlux offices. We are grateful for many fruitful discussions regarding the atmospheric measurements of $CO_2$ at the Risø tall tower and its applications in a modelling framework with Ebba Dellwik at DTU Wind energy.

## References

Ahmadov, R., Gerbig, C., Kretschmer, R., Körner, S., Neininger, B., Dolman, A. J., and Sarrat, C.: Mesoscale covariance of transport and $CO_2$ fluxes: Evidence from observations and simulations using the WRF-VPRM coupled atmosphere-biosphere model, J. Geophys. Res.-Atmospheres, 112, https://doi.org/10.1029/2007JD008552, d22107, 2007.

Ahmadov, R., Gerbig, C., Kretschmer, R., Körner, S., Rödenbeck, C., Bousquet, P., and Ramonet, M.: Comparing high resolution WRF-VPRM simulations and two global CO2 transport models with coastal tower measurements of$CO_2$, Biogeosciences, 6, 807–817, 2009.

Baker, D., Law, R., Gurney, K., Rayner, P., Peylin, P., Denning, A., Bousquet, P., Bruhwiler, L., Chen, Y., Ciais, P., Fung, I., Heimann, M., John, J., Maki, T., Maksyutov, S., Masarie, K., Prather, M., Pak, B., Taguchi, S., and Zhu, Z.: TransCom 3 inversion intercomparison: Impact of transport model errors on the interannual variability of regional $CO_2$ fluxes, 1988-2003, Global Biogeochem. Cy., 20, https://doi.org/10.1029/2004GB002439, 2006.

Bloom, A. A., Exbrayat, J.-F., van der Velde, I. R., Feng, L., and Williams, M.: The decadal state of the terrestrial carbon cycle: Global retrievals of terrestrial carbon allocation, pools, and residence times, PNAS, 113, 1285–1290, https://doi.org/10.1073/pnas.1515160113, 2016.

Brandt, J., Silver, J. D., Frohn, L. M., Geels, C., Gross, A., Hansen, A. B., Hansen, K. M., Hedegaard, G. B., Skjøth, C. A., Villadsen, H., Zare, A., and Christensen, J. H.: An integrated model study for Europe and North America using the Danish Eulerian Hemispheric Model with focus on intercontinental transport of air pollution, Atmos. Environ, 53, 156–176, https://doi.org/10.1016/j.atmosenv.2012.01.011, 2012.

Broquet, G., Chevallier, F., Rayner, P., Aulagnier, C., Pison, I., Ramonet, M., Schmidt, M., Vermeulen, A. T., and Ciais, P.: A European summertime $CO_2$ biogenic flux inversion at mesoscale from continuous in situ mixing ratio measurements, J. Geophys. Res.-Atmospheres, 116, https://doi.org/10.1029/2011JD016202, 2011.

Christensen, J.: The Danish Eulerian hemispheric model - A three-dimensional air pollution model used for the Arctic, Atmos. Environ., 31, 4169–4191, https://doi.org/10.1016/S1352-2310(97)00264-1, 1997.

Christensen, J. H., Brandt, J., Frohn, L. M., and Skov, H.: Modelling of Mercury in the Arctic with the Danish Eulerian Hemispheric Model, Atmos. Chem. Phys., 4, 2251–2257, https://doi.org/10.5194/acp-4-2251-2004, 2004.

Ciais, P., Dolman, A. J., Bombelli, A., Duren, R., Peregon, A., Rayner, P. J., Miller, C., Gobron, N., Kinderman, G., Marland, G., Gruber, N., Chevallier, F., Andres, R. J., Balsamo, G., Bopp, L., Bréon, F.-M., Broquet, G., Dargaville, R., Battin, T. J., Borges, A., Bovensmann, H., Buchwitz, M., Butler, J., Canadell, J. G., Cook, R. B., DeFries, R., Engelen, R., Gurney, K. R., Heinze, C., Heimann, M., Held, A., Henry, M., Law, B., Luyssaert, S., Miller, J., Moriyama, T., Moulin, C., Myneni, R. B., Nussli, C., Obersteiner, M., Ojima, D., Pan, Y., Paris, J.-D., Piao, S. L., Poulter, B., Plummer, S., Quegan, S., Raymond, P., Reichstein, M., Rivier, L., Sabine, C., Schimel, D., Tarasova, O., Valentini, R., Wang, R., van der Werf, G., Wickland, D., Williams, M., and Zehner, C.: Current systematic carbon-cycle observations and the need for implementing a policy-relevant carbon observing system, Biogeosciences, 11, 3547–3602, https://doi.org/10.5194/bg-11-3547-2014, 2014.

Dee, D. P., Uppala, S. M., Simmons, A. J., Berrisford, P., Poli, P., Kobayashi, S., Andrae, U., Balmaseda, M. A., Balsamo, G., Bauer, P., Bechtold, P., Beljaars, A. C. M., van de Berg, L., Bidlot, J., Bormann, N., Delsol, C., Dragani, R., Fuentes, M., Geer, A. J., Haimberger, L., Healy, S. B., Hersbach, H., Hólm, E. V., Isaksen, L., Kållberg, P., Köhler, M., Matricardi, M., McNally, A. P., Monge-Sanz, B. M., Morcrette, J.-J., Park, B.-K., Peubey, C., de Rosnay, P., Tavolato, C., Thépaut, J.-N., and Vitart, F.: The ERA-Interim reanalysis: configuration and performance of the data assimilation system, Q. J. R. Meteorol. Soc., 137, 553–597, https://doi.org/10.1002/qj.828, 2011.

Farquhar, G. D. and von Caemmerer, S.: Modelling of photosynthetic response to the environment, Physiological Plant Ecology II. Encyclopedia of plant physiology, chap. 16, pp. 549–587, Springer-Verlag, 1982.

Gattuso, J., Frankignoulle, M., and Wollast, R.: Carbon and carbonate metabolism in coastal aquatic ecosystems, Annu. Rev. Ecol. syst., 29, 405–434, https://doi.org/10.1146/annurev.ecolsys.29.1.405, 1998.

Geels, C., Christensen, J., Hansen, A., Killsholm, S., Larsen, N., Larsen, S., Pedersen, T., and Sørensen, L.: Modeling concentrations and fluxes of atmospheric $CO_2$ in the North East Atlantic region , Phys. Chem. Earth., 26, 763 – 768, https://doi.org/10.1016/S1464-1909(01)00083-1, 2002.

Geels, C., Doney, S., Dargaville, R., Brandt, J., and Christensen, J.: Investigating the sources of synoptic variability in atmospheric $CO_2$ measurements over the Northern Hemisphere continents: a regional model study, Tellus B, 56, 35–50, 2004.

Geels, C., Andersen, H. V., Skjøth, C. A., Christensen, J. H., Ellermann, T., Løfstrøm, P., Gyldenkærne, S., Brandt, J., Hansen, K. M., Frohn, L. M., and Hertel, O.: Improved modelling of atmospheric ammonia over Denmark using the coupled modelling system DAMOS, Biogeosciences, 9, 2625–2647, https://doi.org/10.5194/bg-9-2625-2012, 2012a.

Geels, C., Hansen, K. M., Christensen, J. H., Skjøth, C. A., Ellermann, T., Hedegaard, G. B., Hertel, O., Frohn, L. M., Gross, A., and Brandt, J.: Projected change in atmospheric nitrogen deposition to the Baltic Sea towards 2020, Atmos. Chem. Phys., 12, 2615–2629, https://doi.org/10.5194/acp-12-2615-2012, 2012b.

Geels, C., Gloor, M., Ciais, P., Bousquet, P., Peylin, P., Vermeulen, A. T., Dargaville, R., Aalto, T., Brandt, J., Christensen, J. H., Frohn, L. M., Haszpra, L., Karstens, U., Rödenbeck, C., Ramonet, M., Carboni, G., and Santaguida, R.: Comparing atmospheric transport models for future regional inversions over Europe - Part 1: mapping the atmospheric $CO_2$ signals, Atmos. Chem. Phys., 7, 3461–3479, 2007.

Gilmanov, T., Soussana, J., Aires, L., Allard, V., Ammann, C., Balzarolo, M., Barcza, Z., Bernhofer, C., Campbell, C., Cernusca, A., Cescatti, A., Clifton-Brown, J., Dirks, B., Dore, S., Eugster, W., Fuhrer, J., Gimeno, C., Gruenwald, T., Haszpra, L., Hensen, A., Ibrom, A., Jacobs, A., Jones, M., Lanigan, G., Laurila, T., Lohila, A., G.Manca, Marcolla, B., Nagy, Z., Pilegaard, K., Pinter, K., Pio, C., Raschi, A., Rogiers, N., Sanz, M., Stefani, P., Sutton, M., Tuba, Z., Valentini, R., Williams, M., and Wohlfahrt, G.: Partitioning European grassland net ecosystem $CO_2$ exchange into gross primary productivity and ecosystem respiration using light response function analysis, Agric. Ecosyst. Environ, 121, 93 – 120, https://doi.org/https://doi.org/10.1016/j.agee.2006.12.008, the Greenhouse Gas Balance of Grasslands in Europe, 2007.

Gurney, K., Law, R., Denning, A., Rayner, P., Baker, D., Bousquet, P., Bruhwiler, L., Chen, Y., Ciais, P., Fan, S., Fung, I., Gloor, M., Heimann, M., Higuchi, K., John, J., Maki, T., Maksyutov, S., Masarie, K., Peylin, P., Prather, M., Pak, B., Randerson, J., Sarmiento, J., Taguchi, S., Takahashi, T., and Yuen, C.: Towards robust regional estimates of $CO_2$ sources and sinks using atmospheric transport models, Nature, 415, 626–630, https://doi.org/10.1038/415626a, 2002.

Gurney, K., Law, R., Denning, A., Rayner, P., Pak, B., Baker, D., Bousquet, P., Bruhwiler, L., Chen, Y., Ciais, P., Fung, I., Heimann, M., John, J., Maki, T., Maksyutov, S., Peylin, P., Prather, M., and Taguchi, S.: Transcom 3 inversion intercomparison: Model mean results for the estimation of seasonal carbon sources and sinks, Global Biogeochem. Cy., 18, https://doi.org/10.1029/2003GB002111, 2004.

Gustafsson, E., Omstedt, A., and Gustafsson, B. G.: The air-water $CO_2$ exchange of a coastal sea - A sensitivity study on factors that influence the absorption and outgassing of $CO_2$ in the Baltic Sea, J. Geophys. Res.-Oceans, 120, 5342–5357, https://doi.org/10.1002/2015JC010832, 2015.

Gypens, N., Lacroix, G., Lancelot, C., and Borges, A. V.: Seasonal and inter-annual variability of air-sea $CO_2$ fluxes and seawater carbonate chemistry in the Southern North Sea, Prog. Oceanogr., 88, 59–77, https://doi.org/10.1016/j.pocean.2010.11.004, 2011.

Hansen, K. M., Christensen, J. H., Brandt, J., Frohn, L. M., and Geels, C.: Modelling atmospheric transport of $\alpha$-hexachlorocyclohexane in the Northern Hemispherewith a 3-D dynamical model: DEHM-POP, Atmos. Chem. Phys., 4, 1125–1137, https://doi.org/10.5194/acp-4-1125-2004, 2004.

Herbst, M., Friborg, T., Ringgaard, R., and Soegaard, H.: Catchment-Wide Atmospheric Greenhouse Gas Exchange as Influenced by Land Use Diversity, Vadose Zone J., 10, 67–77, https://doi.org/10.2136/vzj2010.0058, 2011.

Herbst, M., Friborg, T., Schelde, K., Jensen, R., Ringgaard, R., Vasquez, V., Thomsen, A. G., and Soegaard, H.: Climate and site management as driving factors for the atmospheric greenhouse gas exchange of a restored wetland, Biogeosciences, 10, 39–52, https://doi.org/10.5194/bg-10-39-2013, 2013.

Ho, D. T., Law, C. S., Smith, M. J., Schlosser, P., Harvey, M., and Hill, P.: Measurements of air-sea gas exchange at high wind speeds in the Southern Ocean: Implications for global parameterizations, Geophys. Res. Let., 33, https://doi.org/10.1029/2006GL026817, 2006.

Janssens, I., Freibauer, A., Schlamadinger, B., Ceulemans, R., Ciais, P., Dolman, A., Heimann, M., Nabuurs, G., Smith, P., Valentini, R., and Schulze, E.: The carbon budget of terrestrial ecosystems at country-scale – a European case study, Biogeosciences, 2, 15–26, 2005.

Jepsen, M. R. and Levin, G.: Semantically based reclassification of Danish land-use and land-cover information, Int. J. Geogr. Inf. Sci., 27, 2375–2390, https://doi.org/10.1080/13658816.2013.803555, 2013.

Jones, H. G.: Plants and Microclimate, Cambridge University Press, 1992.

Kattge, J., Diaz, S., Lavorel, S., Prentice, C., Leadley, P., Bönisch, G., Garnier, E., Westoby, M., Reich, P. B., Wright, I. J., Cornelissen, J. H. C., Violle, C., Harrison, S. P., van Bodegom, P. M., Reichstein, M., Enquist, B. J., Soudzilovskaia, N. A., Ackerly, D. D., Anand, M., Atkin, O., Bahn, M., Baker, T. R., Baldocchi, D., Bekker, R., Blanco, C. C., Blonder, B., Bond, W. J., Bradstock, R., Bunker, D. E., Casanoves, F., Cavender-Bares, J., Chambers, J. Q., Chapin, III, F. S., Chave, J., Coomes, D., Cornwell, W. K., Craine, J. M., Dobrin, B. H., Duarte, L., Durka, W., Elser, J., Esser, G., Estiarte, M., Fagan, W. F., Fang, J., Fernández-Méndez, F., Fidelis, A., Finegan, B., Flores, O., Ford, H., Frank, D., Freschet, G. T., Fyllas, N. M., Gallagher, R. V., Green, W. A., Gutierrez, A. G., Hickler, T., Higgins, S. I., Hodgson, J. G., Jalili, A., Jansen, S., Joly, C. A., Kerkhoff, A. J., Kirkup, D., Kitajima, K., Kleyer, M., Klotz, S., Knops, J. M. H., Kramer, K., Kühn, I., Kurokawa, H., Laughlin, D., Lee, T. D., Leishman, M., Lens, F., Lenz, T., Lewis, S. L., Lloyd, J., Llusiá, J., Louault, F., Ma, S., Mahecha, M. D., Manning, P., Massad, T., Medlyn, B. E., Messier, J., Moles, A. T., Müller, S. C., Nadrowski, K., Naeem, S., Niinemets, U., Nöllert, S., Nüske, A., Ogaya, R., Oleksyn, J., Onipchenko, V. G., Onoda, Y., Ordonez, J., Overbeck, G., Ozinga, W. A., Patino, S., Paula, S., Pausas, J. G., Penuelas, J., Phillips, O. L., Pillar, V., Poorter, H., Poorter, L., Poschlod, P., Prinzing, A., Proulx, R., Rammig, A., Reinsch, S., Reu, B., Sack, L., Salgado-Negre, B., Sardans, J., Shiodera, S., Shipley, B., Siefert, A., Sosinski, E., Soussana, J. F., Swaine, E., Swenson, N., Thompson, K., Thornton, P., Waldram, M., Weiher, E., White, M., White, S., Wright, S. J., Yguel, B., Zaehle, S., Zanne, A. E., and Wirth, C.: TRY - a global database of plant traits, Global Change Biol., 17, 2905–2935, https://doi.org/10.1111/j.1365-2486.2011.02451.x, 2011.

Kretschmer, R., Gerbig, C., Karstens, U., Biavati, G., Vermeulen, A., Vogel, F., Hammer, S., and Totsche, K. U.: Impact of optimized mixing heights on simulated regional atmospheric transport of $CO_2$, Atmos. Chem. Phys., 14, 7149–7172, https://doi.org/10.5194/acp-14-7149-2014, 2014.

Kuliński, K. and Pempkowiak, J.: The carbon budget of the Baltic Sea, Biogeosciences, 8, 3219–3230, https://doi.org/10.5194/bg-8-3219-2011, 2011.

Kuss, J., Roeder, W., Wlost, K.-P., and DeGrandpre, M.: Time-series of surface water $CO_2$ and oxygen measurements on a platform in the central Arkona Sea (Baltic Sea): Seasonality of uptake and release, Mar. Chem., 101, 220–232, https://doi.org/http://dx.doi.org/10.1016/j.marchem.2006.03.004, 2006.

Kuznetsov, I. and Neumann, T.: Simulation of carbon dynamics in the Baltic Sea with a 3D model, J. Marine Syst., 111, 167–174, https://doi.org/10.1016/j.jmarsys.2012.10.011, 2013.

Lansø, A. S., Sørensen, L. L., Christensen, J. H., Rutgersson, A., and Geels, C.: The influence of short term variability in surface water $pCO_2$ on the modelled air-sea $CO_2$ exchange, Tellus B, 69, 1302 670, https://doi.org/10.1080/16000889.2017.1302670, 2017.

Lansø, A. S., Bendtsen, J., Christensen, J. H., Sørensen, L. L., Chen, H., Meijer, H. A. J., and Geels, C.: Sensitivity of the air-sea $CO_2$ exchange in the Baltic Sea and Danish inner waters to atmospheric short-term variability, Biogeosciences, 12, 2753–2772, https://doi.org/10.5194/bg-12-2753-2015, 2015.

Lauvaux, T., Schuh, A. E., Uliasz, M., Richardson, S., Miles, N., Andrews, A. E., Sweeney, C., Diaz, L. I., Martins, D., Shepson, P. B., and Davis, K. J.: Constraining the $CO_2$ budget of the corn belt: exploring uncertainties from the assumptions in a mesoscale inverse system, Atmos. Chem. Phys., 12, 337–354, https://doi.org/10.5194/acp-12-337-2012, 2012.

Law, R. M., Peters, W., Rödenbeck, C., Aulagnier, C., Baker, I., Bergmann, D. J., Bousquet, P., Brandt, J., Bruhwiler, L., Cameron-Smith, P. J., Christensen, J. H., Delage, F., Denning, A. S., Fan, S., Geels, C., Houweling, S., Imasu, R., Karstens, U., Kawa, S. R., Kleist, J., Krol, M. C., Lin, S. J., Lokupitiya, R., Maki, T., Maksyutov, S., Niwa, Y., Onishi, R., Parazoo, N., Patra, P. K., Pieterse, G., Rivier, L., Satoh, M., Serrar, S., Taguchi, S., Takigawa, M., Vautard, R., Vermeulen, A. T., and Zhu, Z.: TransCom model simulations of hourly atmospheric $CO_2$: Experimental overview and diurnal cycle results for 2002, Global Biogeochem. Cy., 22, https://doi.org/10.1029/2007GB003050, 2008.

Le Quéré, C., Moriarty, R., Andrew, R. M., Canadell, J. G., Sitch, S., Korsbakken, J. I., Friedlingstein, P., Peters, G. P., Andres, R. J., Boden, T. A., Houghton, R. A., House, J. I., Keeling, R. F., Tans, P., Arneth, A., Bakker, D. C. E., Barbero, L., Bopp, L., Chang, J., Chevallier, F., Chini, L. P., Ciais, P., Fader, M., Feely, R. A., Gkritzalis, T., Harris, I., Hauck, J., Ilyina, T., Jain, A. K., Kato, E., Kitidis, V., Klein Goldewijk, K., Koven, C., Landschützer, P., Lauvset, S. K., Lefèvre, N., Lenton, A., Lima, I. D., Metzl, N., Millero, F., Munro, D. R., Murata, A., Nabel, J. E. M. S., Nakaoka, S., Nojiri, Y., O'Brien, K., Olsen, A., Ono, T., Pérez, F. F., Pfeil, B., Pierrot, D., Poulter, B., Rehder, G., Rödenbeck, C., Saito, S., Schuster, U., Schwinger, J., Séférian, R., Steinhoff, T., Stocker, B. D., Sutton, A. J., Takahashi, T., Tilbrook, B., van der Laan-Luijkx, I. T., van der Werf, G. R., van Heuven, S., Vandemark, D., Viovy, N., Wiltshire, A., Zaehle, S., and Zeng, N.: Global Carbon Budget 2015, Earth System Science Data, 7, 349–396, https://doi.org/10.5194/essd-7-349-2015, 2015.

Le Quéré, C., Andrew, R. M., Friedlingstein, P., Sitch, S., Pongratz, J., Manning, A. C., Korsbakken, J. I., Peters, G. P., Canadell, J. G., Jackson, R. B., Boden, T. A., Tans, P. P., Andrews, O. D., Arora, V. K., Bakker, D. C. E., Barbero, L., Becker, M., Betts, R. A., Bopp, L., Chevallier, F., Chini, L. P., Ciais, P., Cosca, C. E., Cross, J., Currie, K., Gasser, T., Harris, I., Hauck, J., Haverd, V., Houghton, R. A., Hunt, C. W., Hurtt, G., Ilyina, T., Jain, A. K., Kato, E., Kautz, M., Keeling, R. F., Klein Goldewijk, K., Körtzinger, A., Landschützer, P., Lefèvre, N., Lenton, A., Lienert, S., Lima, I., Lombardozzi, D., Metzl, N., Millero, F., Monteiro, P. M. S., Munro, D. R., Nabel, J. E. M. S., Nakaoka, S.-I., Nojiri, Y., Padin, X. A., Peregon, A., Pfeil, B., Pierrot, D., Poulter, B., Rehder, G., Reimer, J., Rödenbeck, C., Schwinger, J., Séférian, R., Skjelvan, I., Stocker, B. D., Tian, H., Tilbrook, B., Tubiello, F. N., van der Laan-Luijkx, I. T., van der Werf, G. R., van Heuven, S., Viovy, N., Vuichard, N., Walker, A. P., Watson, A. J., Wiltshire, A. J., Zaehle, S., and Zhu, D.: Global Carbon Budget 2017, Earth System Science Data, 10, 405–448, https://doi.org/10.5194/essd-10-405-2018, 2018.

Leinweber, A., Gruber, N., Frenzel, H., Friederich, G. E., and Chavez, F. P.: Diurnal carbon cycling in the surface ocean and lower atmosphere of Santa Monica Bay, California, Geophys. Res. Lett., 36, https://doi.org/10.1029/2008GL037018, 2009.

Luyssaert, S., Inglima, I., Jung, M., Richardson, A. D., Reichstein, M., Papale, D., Piao, S. L., Schulzes, E. D., Wingate, L., Matteucci, G., Aragao, L., Aubinet, M., Beers, C., Bernhofer, C., Black, K. G., Bonal, D., Bonnefond, J. M., Chambers, J., Ciais, P., Cook, B., Davis, K. J., Dolman, A. J., Gielen, B., Goulden, M., Grace, J., Granier, A., Grelle, A., Griffis, T., Grünwald, T., Guidolotti, G., Hanson, P. J., Harding, R., Hollinger, D. Y., Hutyra, L. R., Kolar, P., Kruijt, B., Kutsch, W., Lagergren, F., Laurila, T., Law, B. E., Le Maire, G., Lindroth, A., Loustau, D., Malhi, Y., Mateus, J., Migliavacca, M., Misson, L., Montagnani, L., Moncrieff, J., Moors, E., Munger, J. W., Nikinmaa, E., Ollinger, S. V., Pita, G., Rebmann, C., Roupsard, O., Saigusa, N., Sanz, M. J., Seufert, G., Sierra, C., Smith, M. L., Tang, J., Valentini, R., Vesala, T., and Janssens, I. A.: $CO_2$ balance of boreal, temperate, and tropical forests derived from a global database, Global Change Biol., 13, 2509–2537, https://doi.org/10.1111/j.1365-2486.2007.01439.x, 2007.

Meesters, A. G. C. A., Tolk, L. F., Peters, W., Hutjes, R. W. A., Vellinga, O. S., Elbers, J. A., Vermeulen, A. T., van der Laan, S., Neubert, R. E. M., Meijer, H. A. J., and Dolman, A. J.: Inverse carbon dioxide flux estimates for the Netherlands, J. Geophys. Res.-Atmospheres, 117, https://doi.org/10.1029/2012JD017797, 2012.

Mørk, E. T.: Air-Sea exchange of $CO_2$ in coastal waters, Phd thesis, Aarhus University, Department of Bioscience, Denmark, 2015.

Mørk, E. T., Sejr, M. K., Stæhr, P. A., and Sørensen, L. L.: Temporal variability of air-sea $CO_2$ exchange in a low-emission estuary, Estuar. Coast. Shelf. S., 176, 1 – 11, https://doi.org/http://dx.doi.org/10.1016/j.ecss.2016.03.022, 2016.

Nielsen, O.-K., Plejdrup, M., Winther, M., Nielsen, M., Gyldenkærne, S., Mikkelsen, M., Albrektsen, R., Thomsen, M., Hjelgaard, K., Fauser, P., Bruun, H., Johannsen, V., Nord-Larsen, T., Vesterdal, L., Møller, I., Caspersen, O., Rasmussen, E., Petersen, S., Baunbæk, L., and Hansen, M.: Denmark's National Inventory Report 2015. Emission Inventories 1990-2013 – Submitted under the United Nations Framework Convention on Climate Change and the Kyoto Protocol, http://dce2.au.dk/pub/SR171.pdf, 2015.

Norman, M., Parampil, S. R., Rutgersson, A., and Sahlée, E.: Influence of coastal upwelling on the air-sea gas exchange of $CO_2$ in a Baltic Sea Basin, Tellus B, 65, https://doi.org/10.3402/tellusb.v65i0.21831, 2013.

Olivier, J., Janssens-Maenhout, G., Muntean, M., and Peters, J.: Trends in global $CO_2$ emissions: 2014 Report, Report, PBL Netherlands Environmental Assessment Agency, The Hague, 2014.

Omstedt, A., Gustafsson, E., and Wesslander, K.: Modelling the uptake and release of carbon dioxide in the Baltic Sea surface water, Cont. Shelf. Res., 29, 870–885, https://doi.org/10.1016/j.csr.2009.01.006, 2009.

Penning de Vries, F., Jansen, D., ten Berge, H., and Bakema, A.: Simulation of ecophysiological processes of growth in several annual crops. In: Simulation Monographs, Pudoc, Wageningen, 1989.

Peters, W., Jacobson, A., Sweeney, C., Andrews, A., Conway, T., Masarie, K., Miller, J., Bruhwiler, L., Petron, G., Hirsch, A., Worthy, D., van der Werf, G.R.; Randerson, J., Wennberg, P., and Krol, M.C.and Tans, P.: An atmospheric perspective on North American carbon dioxide exchange: CarbonTracker, PNAS, 104, 18 925–18 930, with updates documented at http://carbontracker.noaa.gov, 2007.

Peylin, P., Law, R. M., Gurney, K. R., Chevallier, F., Jacobson, A. R., Maki, T., Niwa, Y., Patra, P. K., Peters, W., Rayner, P. J., Rödenbeck, C., van der Laan-Luijkx, I. T., and Zhang, X.: Global atmospheric carbon budget: results from an ensemble of atmospheric $CO_2$ inversions, Biogeosciences, 10, 6699–6720, https://doi.org/10.5194/bg-10-6699-2013, 2013.

Pilegaard, K., Ibrom, A., Courtney, M. S., Hummelshøj, P., and Jensen, N. O.: Increasing net $CO_2$ uptake by a Danish beech forest during the period from 1996 to 2009, Agr. Forest Meteorol., 151, 934–946, https://doi.org/10.1016/j.agrformet.2011.02.013, 2011.

Plejdrup, M. and Gyldenkærne, S.: Spatial distribution of emissions to air – the SPREAD model, Tech. rep., National Environmental Institute, Aarhus University, 2011.

Pregger, T., Scholz, Y., and Friedrich, R.: Documentation of the Anthropogenic GHG Emission Data for Europe Provided in the Frame of CarboEurope and CarboEurope IP, type, University of Stuttgart, IER -Institute of Energy Economics and the Rational Use of Energy, 2007.

Regnier, P., Friedlingstein, P., Ciais, P., Mackenzie, F. T., Gruber, N., Janssens, I. A., Laruelle, G. G., Lauerwald, R., Luyssaert, S., Andersson, A. J., Arndt, S., Arnosti, C., Borges, A. V., Dale, A. W., Gallego-Sala, A., Goddéris, Y., Goossens, N., Hartmann, J., Heinze, C., Ilyina, T., Joos, F., LaRowe, D. E., Leifeld, J., Meysman, F. J. R., Munhoven, G., Raymond, P. A., Spahni, R., Suntharalingam, P., and Thullner, M.: Anthropogenic perturbation of the carbon fluxes from land to ocean, Nat. Geosci., 6, 597–607, https://doi.org/10.1038/NGEO1830, 2013.

Rödenbeck, C., Gerbig, C., Trusilova, K., and Heimann, M.: A two-step scheme for high-resolution regional atmospheric trace gas inversions based on independent models, Atmos. Chem. Phys., 9, 5331–5342, 2009.

Roobaert, A., Laruelle, G. G., Landschützer, P., and Regnier, P.: Uncertainty in the global oceanic $CO_2$ uptake induced by wind forcing: quantification and spatial analysis, Biogeosciences, 15, 1701–1720, https://doi.org/10.5194/bg-15-1701-2018, 2018.

Sarrat, C., Noilhan, J., Dolman, A. J., Gerbig, C., Ahmadov, R., Tolk, L. F., Meesters, A. G. C. A., Hutjes, R. W. A., Ter Maat, H. W., Perez-Landa, G., and Donier, S.: Atmospheric $CO_2$ modeling at the regional scale: an intercomparison of 5 meso-scale atmospheric models, Biogeosciences, 4, 1115–1126, 2007a.

Sarrat, C., Noilhan, J., Lacarrere, P., Donier, S., Lac, C., Calvet, J. C., Dolman, A. J., Gerbig, C., Neininger, B., Ciais, P., Paris, J. D., Boumard, F., Ramonet, M., and Butet, A.: Atmospheric $CO_2$ modeling at the regional scale: Application to the CarboEurope Regional Experiment, J.Geophys. Res. -Atmospheres, 112, https://doi.org/10.1029/2006JD008107, 2007b.

Skamarock, W. C., Klemp, J. B., Dudhia, J., Gill, D. O., Barker, D. M., Wang, W., and Powers, J. G.: A description of the Advanced Research WRF Version 3, Technical report, NCAR, nCAR Tech Notes-468+STR, 2008.

Skjøth, C. A., Sommer, J., Brandt, J., Hvidberg, M., Geels, C., Hansen, K. M., Hertel, O., Frohn, L. M., and Christensen, J. H.: Copenhagen – a significant source of birch (Betula) pollen?, Int. J. Biometeorol., 52, 453–462, https://doi.org/10.1007/s00484-007-0139-y, 2007.

Smallman, T. L., Moncrieff, J. B., and Williams, M.: WRFv3.2-SPAv2: development and validation of a coupled ecosystem–atmosphere model, scaling from surface fluxes of $CO_2$ and energy to atmospheric profiles, Geosci. Model Dev., 6, 1079–1093, https://doi.org/10.5194/gmd-6-1079-2013, 2013.

Smallman, T. L., Exbrayat, J.-F., Mencuccini, M., Bloom, A. A., and Williams, M.: Assimilation of repeated woody biomass observations constrains decadal ecosystem carbon cycle uncertainty in aggrading forests, J Geophys. Res.-Biogeo., 122, 528–545, https://doi.org/10.1002/2016JG003520, 2017.

Smallman, T. L., Williams, M., and Moncrieff, J. B.: Can seasonal and interannual variation in landscape $CO_2$ fluxes be detected by atmospheric observations of $CO_2$ concentrations made at a tall tower?, Biogeosciences, 11, 735–747, https://doi.org/10.5194/bg-11-735-2014, 2014.

Soegaard, H., Jensen, N., Boegh, E., Hasager, C., Schelde, K., and Thomsen, A.: Carbon dioxide exchange over agricultural landscape using eddy correlation and footprint modelling, Agr. Forest Meteorol., 114, 153–173, https://doi.org/10.1016/S0168-1923(02)00177-6, 2003.

Sogachev, A. and Dellwik, E.: Flux footprints for a tall tower in a land–water mosaic area: A case study of the area around the Risø tower, Agr. Forest Meteorol., 237-238, 326 – 339, https://doi.org/https://doi.org/10.1016/j.agrformet.2017.02.037, 2017.

Sus, O., Williams, M., Bernhofer, C., Béziat, P., Buchmann, N., Ceschia, E., Doherty, R., Eugster, W., Grünwald, T., Kutsch, W., Smith, P., and Wattenbach, M.: A linked carbon cycle and crop developmental model: Description and evaluation against measurements of carbon fluxes and carbon stocks at several European agricultural sites, Agr. Ecosyst. Environ., 139, 402 – 418, https://doi.org/http://dx.doi.org/10.1016/j.agee.2010.06.012, 2010.

Takahashi, T., Sutherland, S., Chipman, D., Goddard, J., Ho, C., Newberger, T., Sweeney, C., and Munro, D.: Climatological distributions of pH, $pCO_2$, total $CO_2$, alkalinity, and $CaCO_3$ saturation in the global surface ocean, and temporal changes at selected locations, Mar. Chem., 164, 95 – 125, https://doi.org/http://dx.doi.org/10.1016/j.marchem.2014.06.004, 2014.

Ter Maat, H. W., Hutjes, R. W. A., Miglietta, F., Gioli, B., Bosveld, F. C., Vermeulen, A. T., and Fritsch, H.: Simulating carbon exchange using a regional atmospheric model coupled to an advanced land-surface model, Biogeosciences, 7, 2397–2417, https://doi.org/10.5194/bg-7-2397-2010, 2010.

Thomas, H.and Bozec, Y., Elkalay, K., and de Baar, H. H. W.: Enhanced open ocean storage of $CO_2$ from shelf Sea Pumping, Science, 304, 1005–1008, 2004.

Tolk, L. F., Dolman, A. J., Meesters, A. G. C. A., and Peters, W.: A comparison of different inverse carbon flux estimation approaches for application on a regional domain, Atmos. Chem. Phys., 11, 10 349–10 365, https://doi.org/10.5194/acp-11-10349-2011, 2011.

Tolk, L. F., Peters, W., Meesters, A. G. C. A., Groenendijk, M., Vermeulen, A. T., Steeneveld, G. J., and Dolman, A. J.: Modelling regional scale surface fluxes, meteorology and $CO_2$ mixing ratios for the Cabauw tower in the Netherlands, Biogeosciences, 6, 2265–2280, 2009.

Uebel, M., Herbst, M., and Bott, A.: Mesoscale simulations of atmospheric $CO_2$ variations using a high-resolution model system with process-based $CO_2$ fluxes, Q. J. Roy. Meteor. Soc., 143, 1860–1876, https://doi.org/10.1002/qj.3047, 2017.

United Nations Chapter XXI: Law of the Sea: title, https://treaties.un.org/Pages/Treaties.aspx?id=21&subid=A&clang=_en, 1984.

Valsala, V. and Murtugudde, R.: Mesoscale and intraseasonal air–sea $CO_2$ exchanges in the western Arabian Sea during boreal summer, Deep-Sea Res. Pt. I, 103, 101 – 113, https://doi.org/http://dx.doi.org/10.1016/j.dsr.2015.06.001, 2015.

Vandemark, D., Salisbury, J. E., Hunt, C. W., Shellito, S. M., Irish, J. D., McGillis, W. R., Sabine, C. L., and Maenner, S. M.: Temporal and spatial dynamics of $CO_2$ air-sea flux in the Gulf of Maine, J. Geophys. Res.-Oceans, 116, https://doi.org/10.1029/2010JC006408, c01012, 2011.

Weiss, R. F.: Carbon Dioxide in Seawater: The Solubility of Non-ideal Gas, Mar. Chem., 2, 203–215, 1974.

Wesslander, K., Omstedt, A., and Schneider, B.: Inter-annual and seasonal variations in the air-sea $CO_2$ balance in the central Baltic Sea and the Kattegat, Cont. Shelf. Res., 30, 1511–1521, https://doi.org/10.1016/j.csr.2010.05.014, 2010.

Wieder, W.: Regridded Harmonized World Soil Database v1.2, https://doi.org/10.3334/ORNLDAAC/1247, http://dx.doi.org/10.3334/ORNLDAAC/1247, 2014.

Williams, M., Rastetter, E. B., Fernandes, D. N., Goulden, M. L., Wofsy, S. C., Shaver, G. R., Melillo, J. M., Munger, J. W., Fan, S.-M., and Nadelhoffer, K. J.: Modelling the soil-plant-atmosphere continuum in a Quercus–Acer stand at Harvard Forest: the regulation of stomatal conductance by light, nitrogen and soil/plant hydraulic properties, Plant Cell Environ., 19, 911–927, https://doi.org/10.1111/j.1365-3040.1996.tb00456.x, 1996.

Williams, M., Malhi, Y., Nobre, A. D., Rastetter, E. B., Grace, J., and Pereira, M. G. P.: Seasonal variation in net carbon exchange and evapotranspiration in a Brazilian rain forest: a modelling analysis, Plant Cell Environ., 21, 953–968, https://doi.org/10.1046/j.1365-3040.1998.00339.x, 1998.

Williams, M., Eugster, W., Rastetter, E. B., Mcfadden, J. P., and Chapin Iii, F. S.: The controls on net ecosystem productivity along an Arctic transect: a model comparison with flux measurements, Global Change Biol., 6, 116–126, https://doi.org/10.1046/j.1365-2486.2000.06016.x, 2000.

Williams, M., Schwarz, P. A., Law, B. E., Irvine, J., and Kurpius, M. R.: An improved analysis of forest carbon dynamics using data assimilation, Global Change Biol., 11, 89–105, https://doi.org/10.1111/j.1365-2486.2004.00891.x, 2005.

Williams, M., Law, B., Anthoni, P., and Unsworth, M.: Use of a simulation model and ecosystem flux data to examine carbon-water interactions in ponderosa pine, Tree Physiol., 21, 287–298, 2001.

Wullschleger, S. D.: Biochemical Limitations to Carbon Assimilation in C3 Plants – A Retrospective Analysis of the A/Ci Curves from 109 Species, J. Exp. Bot., 44, 907–920, https://doi.org/10.1093/jxb/44.5.907, 1993.

Zare, A., Christensen, J. H., Gross, A., Irannejad, P., Glasius, M., and Brandt, J.: Quantifying the contributions of natural emissions to ozone and total fine PM concentrations in the Northern Hemisphere, Atmos. Chem. Phys., 14, 2735–2756, https://doi.org/10.5194/acp-14-2735-2014, 2014.

Zscheischler, J., Mahecha, M. D., Avitabile, V., Calle, L., Carvalhais, N., Ciais, P., Gans, F., Gruber, N., Hartmann, J., Herold, M., Ichii, K., Jung, M., Landschützer, P., Laruelle, G. G., Lauerwald, R., Papale, D., Peylin, P., Poulter, B., Ray, D., Regnier, P., Rödenbeck, C., Roman-Cuesta, R. M., Schwalm, C., Tramontana, G., Tyukavina, A., Valentini, R., van der Werf, G., West, T. O., Wolf, J. E., and Reichstein, M.: Reviews and syntheses: An empirical spatiotemporal description of the global surface–atmosphere carbon fluxes: opportunities and data limitations, Biogeosciences, 14, 3685–3703, https://doi.org/10.5194/bg-14-3685-2017, 2017.

Biogeosciences Discuss., https://doi.org/10.5194/bg-2018-240
Manuscript under review for journal Biogeosciences
Discussion started: 27 June 2018


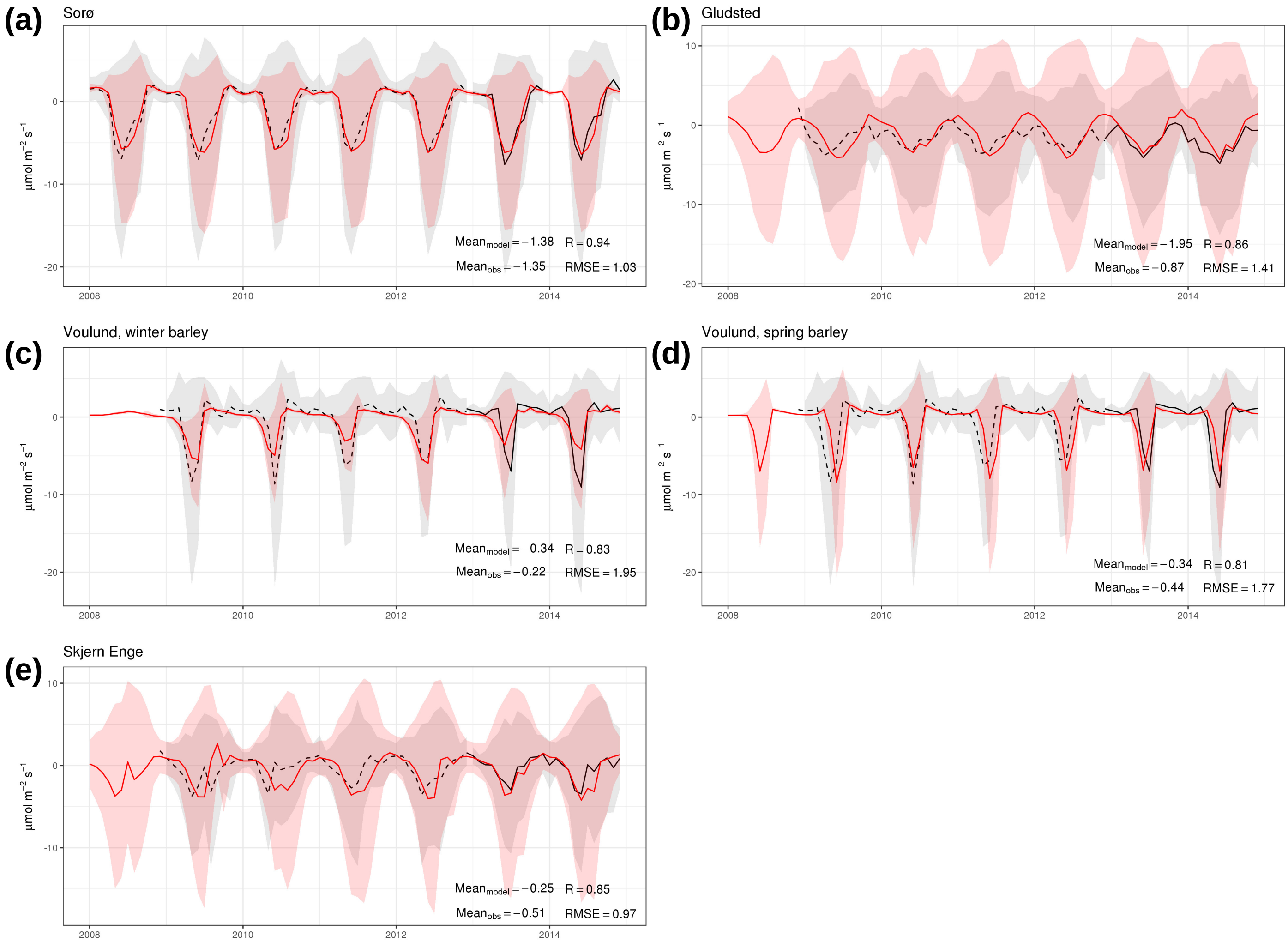


**Figure 1.** Monthly averaged values of observed (black dashed, calibration period; black solid, validation period) and simulated (red) net ecosystem exchange (NEE) plotted together with standard deviations (shaded area) for the Danish flux sites with measurements in the simulation period. The model mean ($\text{Mean}_{model}$), observational mean ($\text{Mean}_{obs}$), correlation (R) and root mean square error (RMSE) for the validation period (2013 and 2014) are shown for each site.

Biogeosciences Discuss., https://doi.org/10.5194/bg-2018-240
Manuscript under review for journal Biogeosciences
Discussion started: 27 June 2018


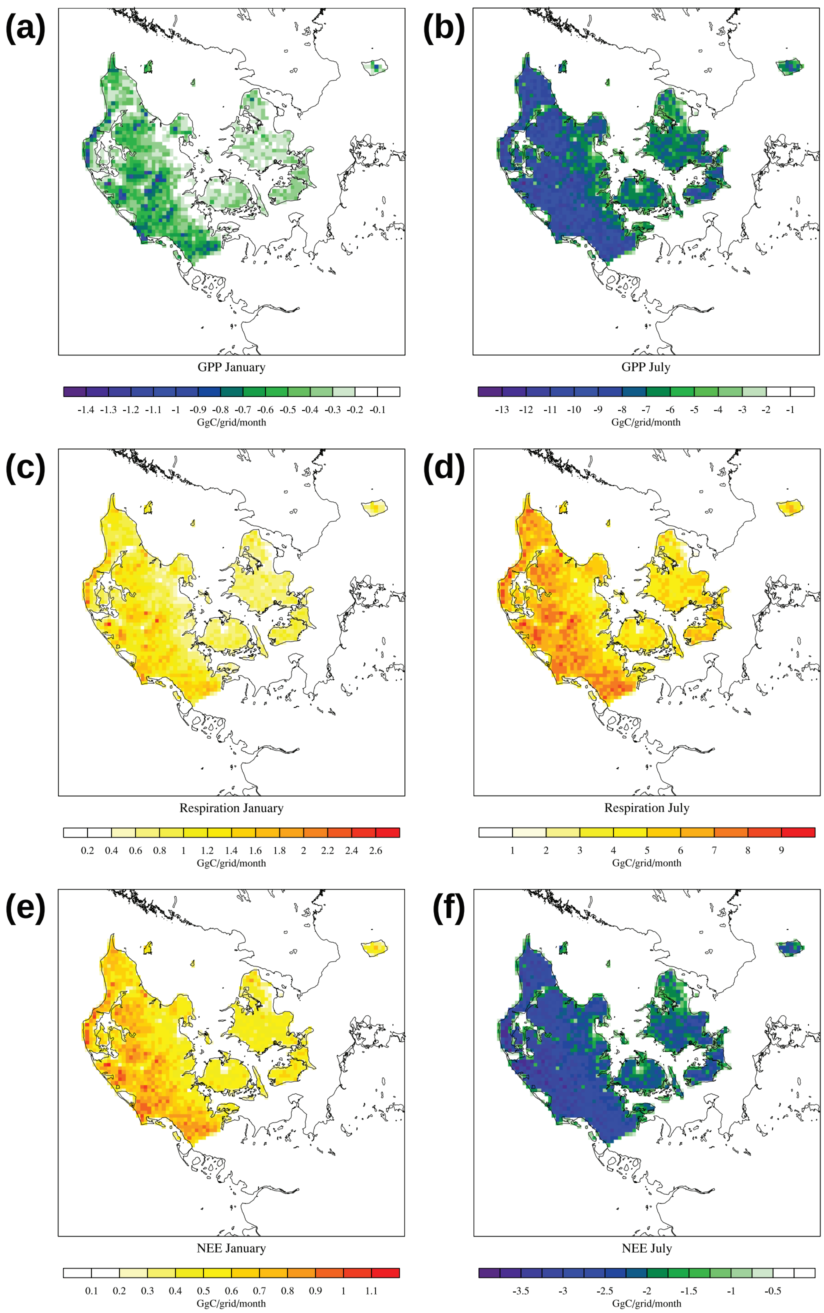


**Figure 2. (a, b)** 2011 January and July gross primary productivity (GPP), **(c, d)** 2011 January and July respiration including autotrophic and heterotrophic respiration, **(e, f)** 2011 January and July NEE.

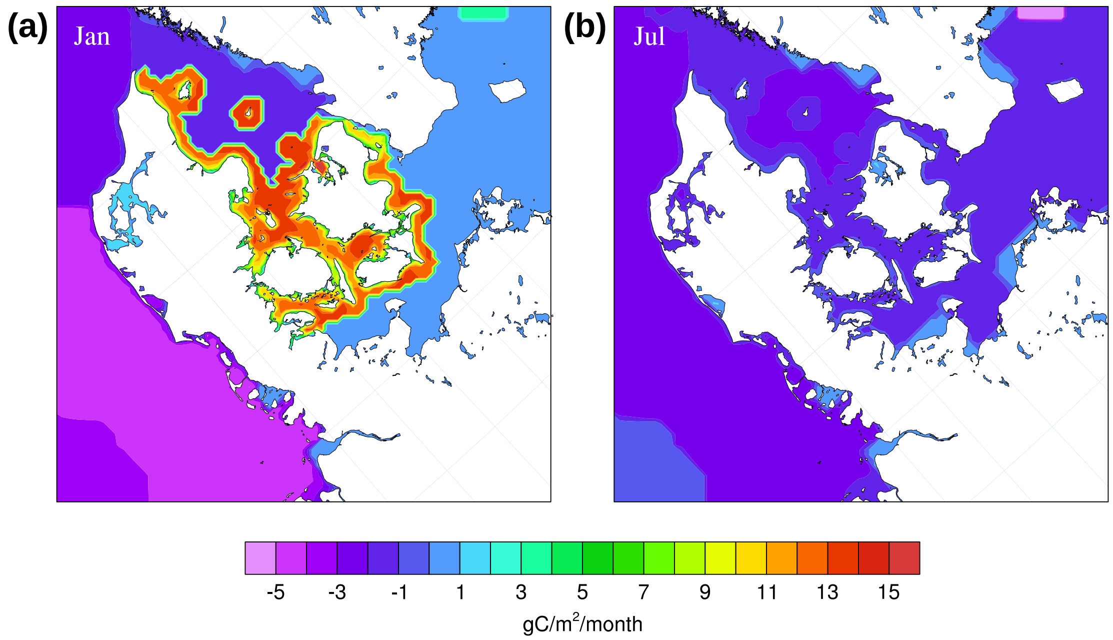


**Figure 3.** Simulated air-sea $CO_2$ exchange for January **(a)** and July **(b)** 2011.

Biogeosciences Discuss., https://doi.org/10.5194/bg-2018-240
Manuscript under review for journal Biogeosciences
Discussion started: 27 June 2018


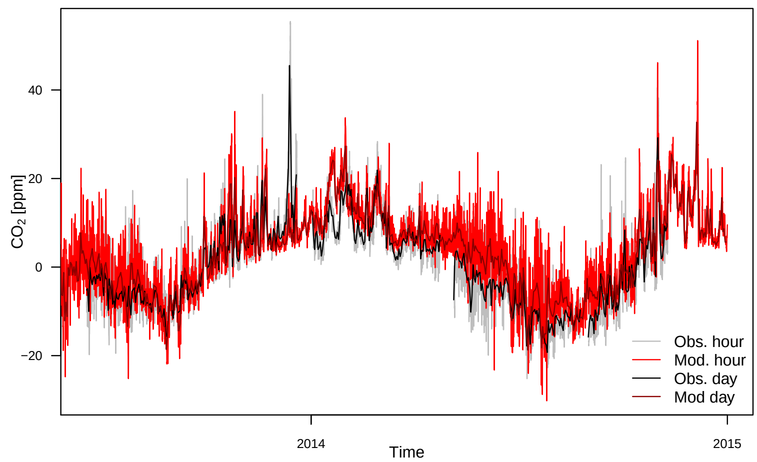


**Figure 4.** One-hour averages and daily averages of modelled and continuously measured atmospheric $CO_2$ at the Risø site for 2013-2014. The annual mean values have been removed from the time series.

Biogeosciences Discuss., https://doi.org/10.5194/bg-2018-240
Manuscript under review for journal Biogeosciences
Discussion started: 27 June 2018


Biogeosciences
Discussions
Open Access

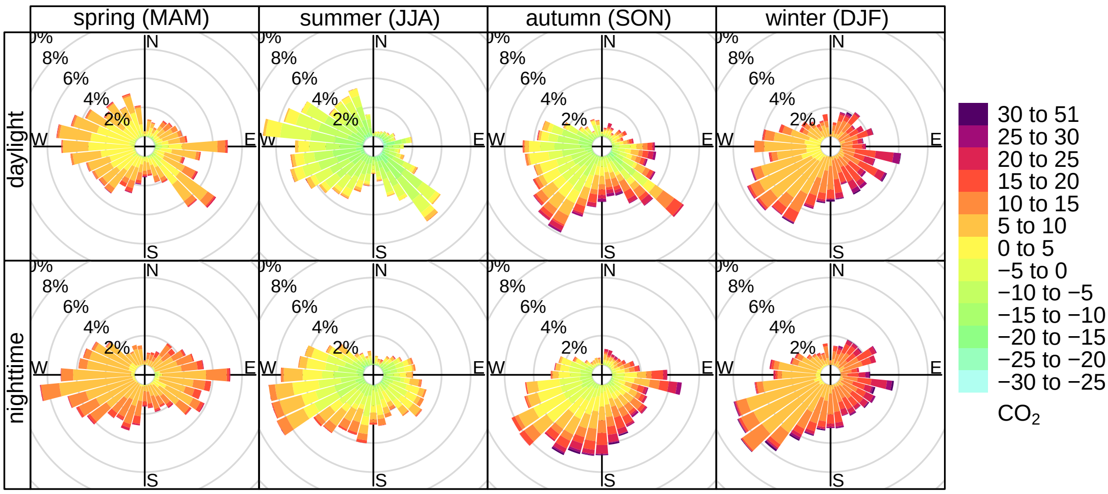


**Figure 5.** Concentration roses of modelled atmospheric $CO_2$ [ppm] at the Risø site for 2011-2014. The wind direction is split into 10° intervals and the frequency indicated by the concentric circles. The colours indicate the $CO_2$ concentrations with mean removed that have been transported to the site from the given wind directions.

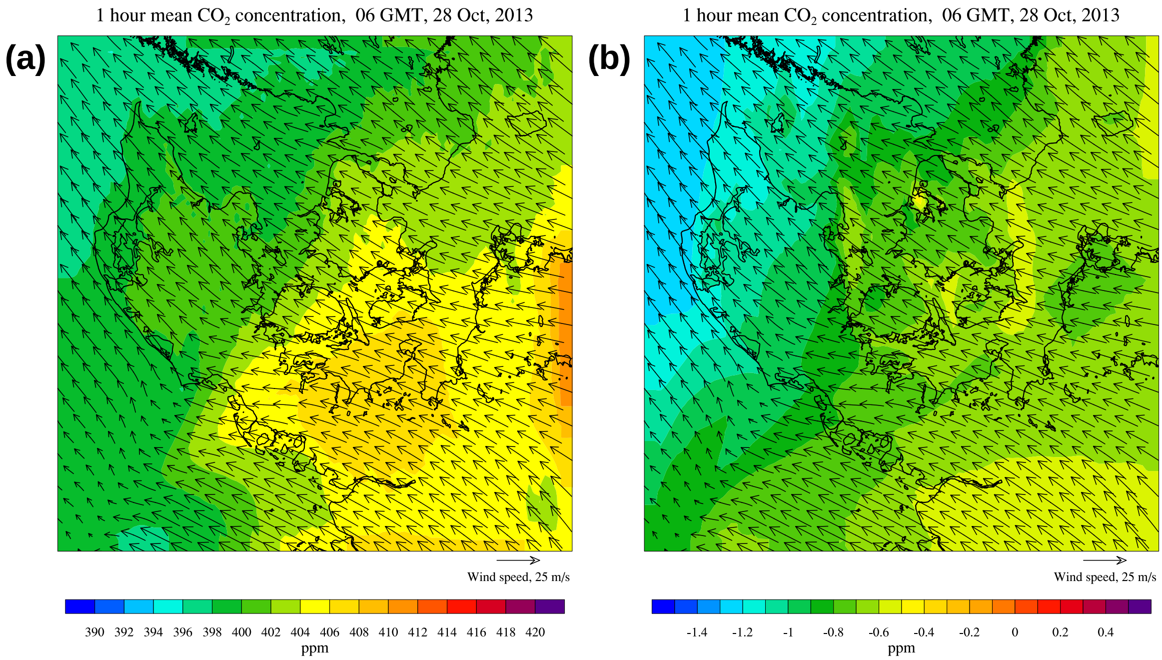


**Figure 6. (a)** Atmospheric $CO_2$ concentrations including the annual background across Denmark 28 October 2013 06 UTC during the October storm. **(b)** The contribution to the atmospheric $CO_2$ concentration alone from marine exchange 28 October 2013 06 UTC. The less negative values at the Roskilde Fjord system indicates release of $CO_2$ to the atmosphere.

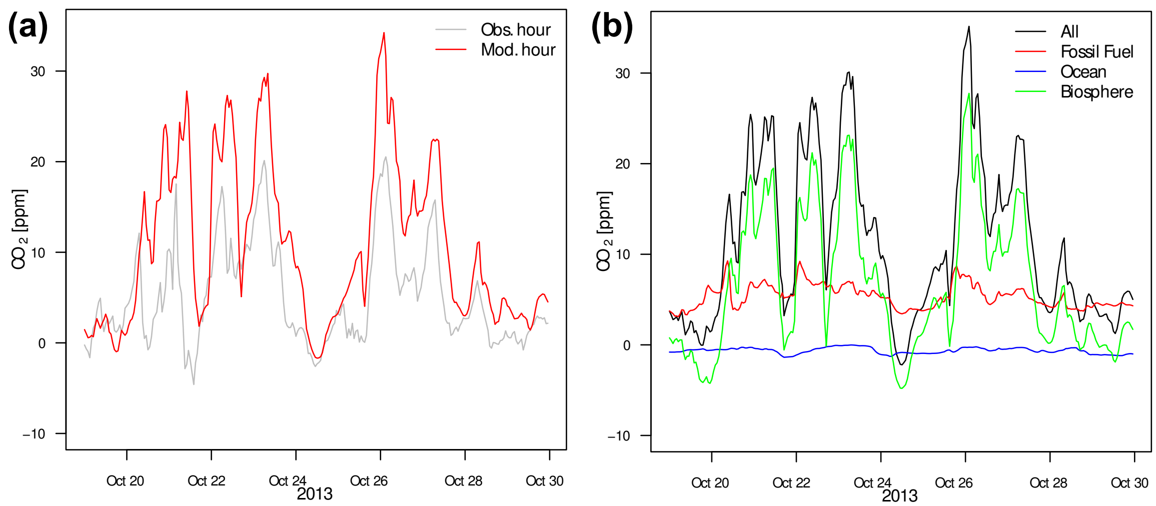


**Figure 7.** **(a)** One-hour averages of modelled and continuously measured atmospheric $CO_2$ at the Risø site for 19-29 October 2013 with annual means removed. **(b)** Contributions from fossil fuel emission, oceanic surface exchange and biospheric surface exchange to the atmospheric $CO_2$ concentration, shown as one-hour averages of modelled concentrations at the Risø site for 19-29 October 2013

Biogeosciences Discuss., https://doi.org/10.5194/bg-2018-240
Manuscript under review for journal Biogeosciences
Discussion started: 27 June 2018



**Figure A1.** Square kilometers of the seven land-use classification contained in each model grid.

Biogeosciences Discuss., https://doi.org/10.5194/bg-2018-240
Manuscript under review for journal Biogeosciences
Discussion started: 27 June 2018


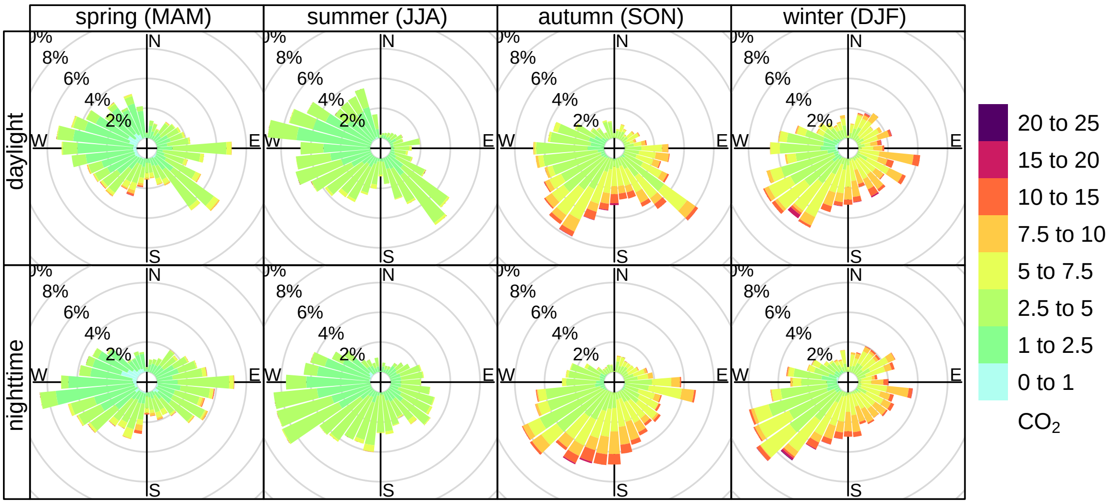


**Figure C1.** Concentration roses of the fossil fuel emission contribution to the modelled atmospheric $CO_2$ [ppm] at the Risø site for 2011-2014. The wind direction is split into 10° intervals and the frequency indicated by the concentric circles. The colours indicate the $CO_2$ contribution that have been transported to the site from the given wind directions.

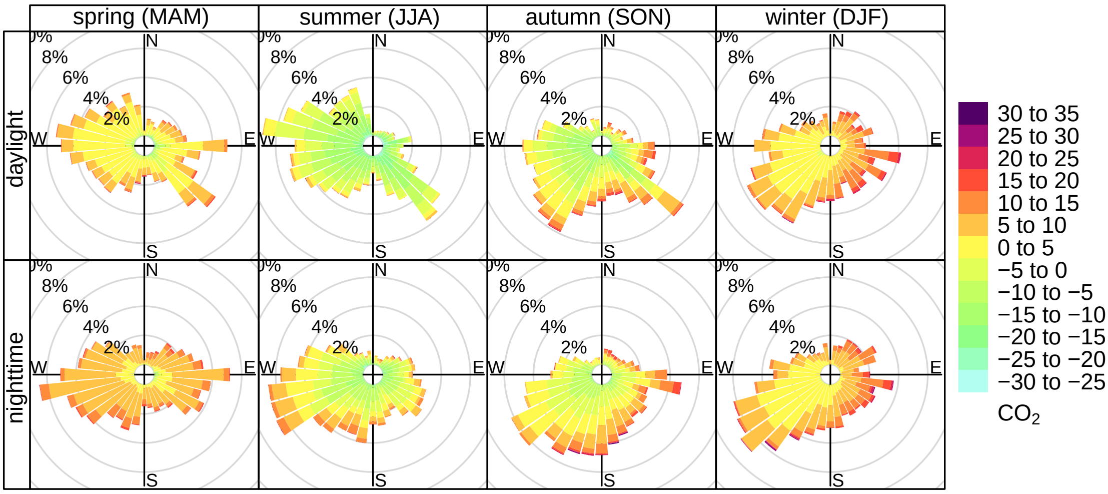


**Figure C2.** Concentration roses of the biospheric contribution to the modelled atmospheric $CO_2$ [ppm] at the Risø site for 2011-2014. The wind direction is split into 10° intervals and the frequency indicated by the concentric circles. The colours indicate the $CO_2$ contribution that have been transported to the site from the given wind directions.

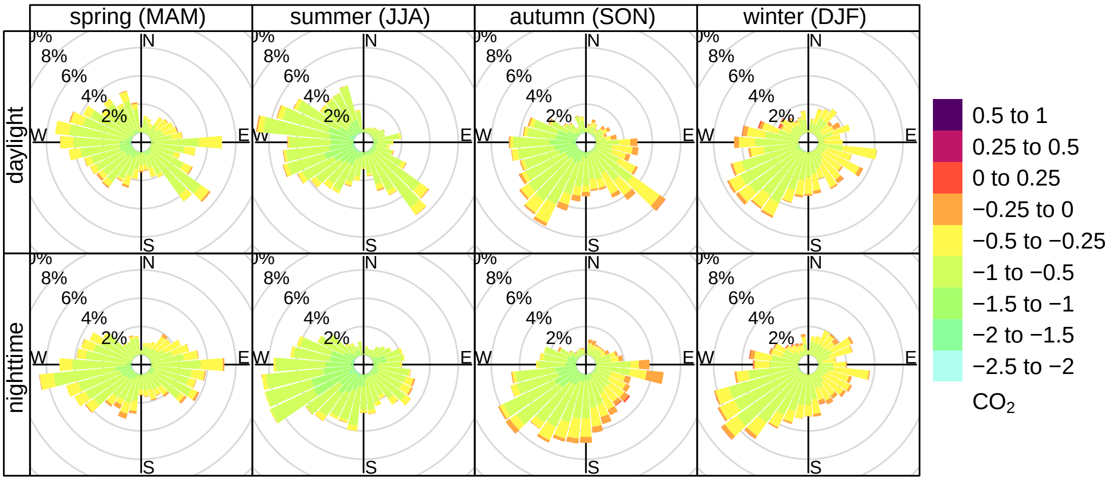


**Figure C3.** Concentration roses of the oceanic contribution to the modelled atmospheric $CO_2$ [ppm] at the Risø site for 2011-2014. The wind direction is split into 10° intervals and the frequency indicated by the concentric circles. The colours indicate the $CO_2$ contribution that have been transported to the site from the given wind directions.

Biogeosciences Discuss., https://doi.org/10.5194/bg-2018-240
Manuscript under review for journal Biogeosciences
Discussion started: 27 June 2018


**Table 1.** Location, species, land-use classification in the model system for the five Danish Eddy Covariance (EC) sites used for calibration and validation of the SPA model.

| Site | Location | Calibration | Validation | Species | LU in SPA-DEHM | Reference |
|---|---|---|---|---|---|---|
| Gludsted | 56°04′ N, 9°20′ E | 2009-2012 | 2013-2014 | Norway Spruce | Evergreen forest | HOBE |
| Risbyholm | 55°32′ N, 12°06′ E | 2004-2008 | - | Winter Wheat | Winter wheat and winter crops | Fluxnet |
| Skjern Enge | 55°55′ N, 8°24′ E | 2009-2012 | 2013-2014 | Grass | Grassland | HOBE |
| Sorø | 55°29′ N, 11°39′ E | 2006-2012 | 2013-2014 | Beech | Deciduous forest | Fluxnet |
| Voulund | 56°02′ N, 9°09′ E | 2009-2012 | 2013-2014 | Spring and winter barley | Spring/winter barley | HOBE |

Biogeosciences Discuss., https://doi.org/10.5194/bg-2018-240
Manuscript under review for journal Biogeosciences
Discussion started: 27 June 2018


**Table 2.** Percentage of monthly GPP from each land-use class to the total monthly GPP for Denmark during 2011.

| | Area [km$^2$] | Jan | Feb | Mar | Apr | May | Jun | Jul | Aug | Sep | Oct | Nov | Dec |
|---|---|---|---|---|---|---|---|---|---|---|---|---|---|
| Deciduous | 3,358 | 0.2 | 0.3 | 0.3 | 5.1 | 8.1 | 7.0 | 7.2 | 11.0 | 8.9 | 5.1 | 1.5 | 0.4 |
| Evergreen | 1,870 | 21.4 | 24.8 | 24.5 | 17.5 | 11.4 | 7.8 | 7.8 | 12.5 | 13.5 | 14.4 | 15.0 | 16.1 |
| Winter Wheat | 9,269 | 1.8 | 3.9 | 9.6 | 15.0 | 22.1 | 24.4 | 23.8 | 2.4 | 0.0 | 0.7 | 4.2 | 6.8 |
| Winter barley | 1,211 | 0.1 | 0.3 | 0.8 | 1.4 | 2.3 | 1.9 | 0.6 | 0.0 | 0.0 | 0.1 | 0.4 | 0.6 |
| Spring crops | 5,368 | 0.0 | 0.0 | 0.0 | 1.8 | 9.0 | 18.5 | 16.1 | 0.0 | 0.0 | 0.0 | 0.0 | 0.0 |
| Grassland | 6,924 | 48.8 | 45.2 | 41.4 | 37.8 | 30.0 | 25.8 | 28.5 | 47.3 | 49.3 | 50.6 | 49.6 | 48.3 |
| Agr. Other | 3,909 | 27.7 | 25.7 | 23.4 | 21.5 | 17.1 | 14.7 | 15.9 | 26.7 | 28.3 | 29.0 | 29.2 | 27.8 |

Biogeosciences Discuss., https://doi.org/10.5194/bg-2018-240
Manuscript under review for journal Biogeosciences
Discussion started: 27 June 2018


**Table 3.** Percentage of monthly respiration from each land-use class to the total monthly respiration for Denmark during 2011.

| | Area [km$^2$] | Jan | Feb | Mar | Apr | May | Jun | Jul | Aug | Sep | Oct | Nov | Dec |
|---|---|---|---|---|---|---|---|---|---|---|---|---|---|
| Deciduous | 3,358 | 6.0 | 5.2 | 4.3 | 5.6 | 5.7 | 5.1 | 5.0 | 7.0 | 7.7 | 6.9 | 7.0 | 6.6 |
| Evergreen | 1,870 | 13.5 | 15.7 | 17.4 | 14.9 | 12.3 | 9.5 | 8.8 | 11.5 | 11.7 | 11.0 | 10.6 | 11.2 |
| Winter Wheat | 9,269 | 13.1 | 11.9 | 12.1 | 13.5 | 18.5 | 21.8 | 21.6 | 8.5 | 6.5 | 12.5 | 15.0 | 14.2 |
| Winter barley | 1,211 | 1.3 | 1.2 | 1.2 | 1.4 | 2.0 | 1.9 | 1.0 | 0.6 | 0.6 | 1.3 | 1.5 | 1.5 |
| Spring crops | 5,368 | 4.8 | 4.2 | 3.8 | 6.3 | 7.8 | 12.8 | 14.4 | 4.7 | 4.9 | 4.9 | 5.4 | 5.6 |
| Grassland | 6,924 | 39.5 | 39.6 | 39.1 | 37.3 | 34.3 | 31.2 | 31.6 | 43.3 | 43.7 | 40.6 | 38.6 | 38.9 |
| Agr. Other | 3,909 | 22.0 | 22.2 | 22.0 | 21.0 | 19.5 | 17.7 | 17.7 | 24.4 | 24.9 | 23.0 | 21.9 | 22.0 |

Biogeosciences Discuss., https://doi.org/10.5194/bg-2018-240
Manuscript under review for journal Biogeosciences
Discussion started: 27 June 2018


**Table B1.** Monthly gross primary production (GPP) for Denmark [GgC/month] as simulated by each of the seven land-use classes.

| | Jan | Feb | Mar | Apr | May | Jun | Jul | Aug | Sep | Oct | Nov | Dec |
|---|---|---|---|---|---|---|---|---|---|---|---|---|
| Deciduous | -1 | -2 | -4 | -185 | -629 | -869 | -853 | -710 | -378 | -120 | -14 | -2 |
| Evergreen | -124 | -193 | -379 | -640 | -881 | -970 | -919 | -809 | -571 | -340 | -134 | -94 |
| Winter Wheat | -11 | -30 | -148 | -550 | -1714 | -3042 | -2801 | -157 | 0 | -18 | -38 | -40 |
| Winter barley | -1 | -2 | -13 | -53 | -179 | -234 | -72 | 0 | 0 | -2 | -3 | -3 |
| Spring crops | 0 | 0 | 0 | -65 | -702 | -2315 | -1903 | 0 | 0 | 0 | 0 | 0 |
| Grassland | -282 | -353 | -640 | -1385 | -2327 | -3223 | -3365 | -3053 | -2083 | -1195 | -444 | -283 |
| Agr. Other | -160 | -201 | -362 | -786 | -1324 | -1829 | -1877 | -1722 | -1196 | -684 | -262 | -163 |
| ALL | -579 | -781 | -1546 | -3665 | -7756 | -12482 | -11789 | -6451 | -4228 | -2360 | -894 | -586 |

Biogeosciences Discuss., https://doi.org/10.5194/bg-2018-240
Manuscript under review for journal Biogeosciences
Discussion started: 27 June 2018

Biogeosciences
Discussions
Open Access

**Table B2.** Monthly respiration for Denmark [GgC/month] as simulated by each of the seven land-use classes

| | Jan | Feb | Mar | Apr | May | Jun | Jul | Aug | Sep | Oct | Nov | Dec |
|---|---|---|---|---|---|---|---|---|---|---|---|---|
| Deciduous | 87 | 73 | 91 | 215 | 318 | 395 | 406 | 390 | 322 | 217 | 134 | 113 |
| Evergreen | 196 | 221 | 364 | 572 | 689 | 742 | 711 | 640 | 490 | 343 | 206 | 192 |
| Winter Wheat | 190 | 168 | 254 | 519 | 1032 | 1698 | 1751 | 470 | 271 | 390 | 289 | 244 |
| Winter barley | 19 | 16 | 25 | 53 | 110 | 145 | 80 | 34 | 26 | 39 | 29 | 25 |
| Spring crops | 69 | 60 | 79 | 240 | 437 | 999 | 1168 | 260 | 205 | 152 | 105 | 96 |
| Grassland | 576 | 558 | 819 | 1429 | 1915 | 2433 | 2562 | 2405 | 1829 | 1269 | 747 | 668 |
| Agr. Other | 320 | 313 | 461 | 807 | 1090 | 1382 | 1435 | 1357 | 1044 | 719 | 423 | 377 |
| ALL | 1458 | 1410 | 2094 | 3835 | 5590 | 7795 | 8113 | 5556 | 4188 | 3129 | 1933 | 1715 |

Biogeosciences Discuss., https://doi.org/10.5194/bg-2018-240
Manuscript under review for journal Biogeosciences
Discussion started: 27 June 2018


Biogeosciences
Discussions
Open Access

**Table B3.** Monthly net ecosystem exchange (NEE) for Denmark [GgC/month] as simulated by each of the seven land-use classes

| | Jan | Feb | Mar | Apr | May | Jun | Jul | Aug | Sep | Oct | Nov | Dec |
|---|---|---|---|---|---|---|---|---|---|---|---|---|
| Deciduous | 86 | 71 | 87 | 30 | -311 | -474 | -447 | -320 | -56 | 97 | 121 | 111 |
| Evergreen | 73 | 28 | -15 | -68 | -192 | -228 | -208 | -169 | -81 | 3 | 72 | 98 |
| Winter Wheat | 180 | 137 | 106 | -30 | -682 | -1344 | -1050 | 313 | 271 | 372 | 251 | 204 |
| Winter barley | 18 | 14 | 12 | 0 | -69 | -89 | 8 | 34 | 26 | 37 | 26 | 21 |
| Spring crops | 69 | 60 | 79 | 175 | -265 | -1316 | -734 | 260 | 205 | 152 | 105 | 96 |
| Grassland | 294 | 205 | 180 | 44 | -412 | -791 | -803 | -647 | -254 | 74 | 303 | 385 |
| Agr. Other | 160 | 113 | 99 | 20 | -235 | -447 | -442 | -365 | -153 | 35 | 161 | 214 |
| ALL | 880 | 628 | 548 | 170 | -2166 | -4687 | -3676 | -895 | -41 | 769 | 1038 | 1129 |